https://doi.org/10.5194/hess-2020-606
Preprint. Discussion started: 4 December 2020


Hydrology and Earth System Sciences
Discussions

# Uncertainties and their interaction in flood risk assessment with climate change

Hadush Meresa[1], Conor Murphy[1], Rowan Fealy[1], Saeed Golian[1]

[1]Irish Climate Analysis and Research UnitS (ICARUS), Dept. of Geography, Maynooth University, Maynooth, Ireland.
*Correspondence to*: Hadush Meresa (Hadush.Meresa@mu.ie)

**Abstract**

The assessment of future impacts of climate change is associated with a cascade of uncertainty linked to the modelling chain employed in assessing local scale changes. Understanding and quantifying this cascade is essential to developing effective adaptation actions. We evaluate and quantify uncertainties in future flood quantiles associated with climate change for four Irish catchments, incorporating within our modelling chain uncertainties associated with 12 Global Climate Models contained in the Coupled Model Intercomparison Project Phase 6, five different bias correction approaches, hydrological model parameter uncertainty and use of three different extreme value distributions for flood frequency analysis. Results indicate increased flood risk in all catchments for different Shared Socioeconomic Pathways (SSPs), with changes in flooding related to changes in annual maximum precipitation. We use a sensitivity test based on the analysis of variance (ANOVA) to decompose uncertainties and their interactions in estimating selected flood quantiles in the 2080s for each catchment. We find that the dominant sources of uncertainty vary between catchments, calling into question the ability to generalise about the importance of different components of the cascade of uncertainty in future flood risk. For two of our catchments, uncertainties associated with bias correction methods and extreme value distributions outweigh the uncertainty associated with the ensemble of climate models. For all catchments and flood quantiles examined, hydrological model parameter uncertainty is the least important component of our modelling chain, while the uncertainties derived from the interaction of components are substantial (>20 percent of overall uncertainty in two catchments). While our sample is small, there is evidence that the dominant components of the cascade of uncertainty may be linked to catchment characteristics and rainfall runoff processes. Future work that seeks to further explore the dominant components of uncertainty as they relate to catchment characteristics may provide insight into a priori identifying the key components of modelling chains to be included in climate change impact assessments.

**Keywords:** modelling, flood, climate change, uncertainty, impact, bias correction, GLUE, GR4J

https://doi.org/10.5194/hess-2020-606
Preprint. Discussion started: 4 December 2020


Hydrology and Earth System Sciences
Discussions

## 1 Introduction

Climate change is likely to increasingly affect hydrological regimes and flood hazards over coming decades. Significant changes in atmospheric temperature, precipitation, humidity, and circulation are expected, which may result in increasing extreme events, including floods (IPCC, 2013). According to Rojas et al. (2013), flood frequency in Europe will increase due to climate change, with significant socio-economic implications for the region. Blöschl et al., (2017) and Blöschl et al., (2019) conclude that the timing and magnitude of European floods are shifting due to climate change and its consequences are not uniform across the region, with north western Europe experiencing earlier and higher flood peaks. Modelling and understanding of catchment scale flood risk projections is therefore an important endeavour for informing adaptation strategies.

However, this task is subject to considerable uncertainties (Wilby and Dessai, 2010; Smith et al., 2018). Traditional or top-down climate change impact assessments typically follow a modelling chain where output from Global Climate Models (GCMs), forced with estimates of future greenhouse gas concentrations, are extracted, and scaled to represent a study catchment. Hydrological models, calibrated for current conditions, are then forced with these GCM outputs to create discharge series spanning multiple decades into the future. When assessing flood risk, extreme value distributions are typically fitted to samples of extreme events (e.g. annual maximum flood series) representing current and future climates to evaluate changes in the characteristics of flooding. This modelling chain is replete with uncertainties that propagate and interact, resulting in large ranges of change at the catchment scale (e.g. Meresa, 2019) that can impede decision making (Smith et al., 2018). Over recent decades many studies have attempted to quantify the uncertainties in future climate change impacts due to the use of different climate models (e.g Knutti & Sedláček, 2013), natural variability (e.g. Hughes et al., 2011), bias correction techniques (e.g. Kay et al., 2009; Saini et al., 2015; Soriano et al., 2019), downscaling approaches (e.g. Fowler et al., 2007; Gutmann et al., 2014), hydrological modelling uncertainties (e.g. Wilby & Harris, 2006; Bastola et al., 2011; Meresa & Romanowicz, 2017; Broderick et al., 2019) and the application of different extreme value distributions for flood risk estimation (e.g. Meresa & Romanowicz, 2017; Lawrence, 2020).

Recognition of the uncertainties inherent in future climate risk have also given rise to novel approaches to decision-making that embrace uncertainties (e.g. Wilby & Murphy, 2019; Clark et al., 2016). Rather than aiming to derive precise assessments of future risk, such approaches aim to stress test and evaluate adaptation options, in static or dynamic ways (Mazzorana et al., 2012), to identify actions that are functional across a range of plausible future conditions, rather than optimised to a certain outcome (e.g. structured decision making (SDM), robust decision making, decision scaling, adaptation pathways). Each of these approaches require the cascade of uncertainty to be evaluated or navigated in ways that can better inform adaptation. For example, in Ireland Broderick et al. (2019) employ a scenario neutral framework ( Prudhomme et al., 2011) to evaluate design allowances for flood defences taking into account uncertainties derived from a large climate model ensemble, natural variability and hydrological models.

https://doi.org/10.5194/hess-2020-606
Preprint. Discussion started: 4 December 2020


Hydrology and Earth System Sciences
Discussions

Whether employing traditional impact led or novel decision centric approaches, it is critical that key components of the cascade of uncertainty are adequately included. Research over the past two decades clearly shows that methodological choices made in assessing future climate change fundamentally impact on the portrayal of climate risk (Clark et al., 2016; Melsen et al., 2019). Moreover, deep uncertainty can arise by virtue of the ad-hoc ways in which components of possible modelling chains are assembled and characterised within the overall modelling framework adopted (Wilby and Murphy 2019). Yet there are no established ways of sampling from the hierarchy of models used to evaluate impacts of climate change (Clark et al., 2016). Therefore, an important step in better integrating future climate risk into decision-making is the development of techniques that allow the contribution of different components of uncertainty and their interactions to be quantified and partitioned to help scientists and decision makers better navigate the cascade of uncertainty. In this regard ANOVA (ANalysis Of Variance) based techniques, which can be used to decompose sources of uncertainty and their interaction, offer significant utility (e.g. Kay et al., 2009;Vetter et al., 2016; Hattermann et al., 2018; Meresa, 2020).

In this study, we explore uncertainties in future flood risk for four Irish catchments and employ variance decomposition to quantify the contribution of various sources of uncertainty, together with their interaction, to the overall uncertainty in flood risk. In doing so we place emphasis on evaluating the uncertainties derived from; i) climate models in the newly available Coupled Model Inter-comparison Project Phase 6 (CMIP6) ensemble (Wyser et al., 2019); ii) widely used bias correction techniques; iii) hydrological model parameter uncertainty, and iv) the use of different extreme value distributions. The remainder of the paper is organised as follows; Section 2 outlines the study design and data/methods employed, Section 3 presents key results, exploring uncertainties for key steps in the modelling chain examined, together with their contributions and interactions to the full range of project change in flood risk. Section 4 provides a discussion of key insights, limitations and future directions before drawing main conclusions in Section 5.

## 2 Modelling and numerical experiments

Our study design is illustrated in Figure 1. We quantify uncertainties and their interaction in projected flood hazards using 12 Global Climate Models (GCMs) contained in the Coupled Model Inter-comparison Project Phase 6 (CMIP6) ensemble (https://esgf-node.llnl.gov/search/cmip6/), forced using three Shared Socioeconomic Pathways (SSP) scenarios. We use five bias correction techniques (Change factor (CF), Double Gamma Distribution Quantile (DGQM), Birnbaum distribution Quantile mapping (BQM), Single Gamma Distribution Quantile (SGQM), and Empirical Quantile (EQM)) to post-process climate model outputs (daily precipitation and air temperature time series). The daily bias corrected precipitation and temperature data are used as input to the Génie Rural à 4 paramètres Journalier (GR4J) hydrological model (Perrin et al., 2003). GR4J has been previously applied to simulate high flows in Ireland, showing good performance in capturing a range of hydrological signatures across diverse catchments (Broderick et al., 2019). The Generalized Likelihood Uncertainty Estimation

https://doi.org/10.5194/hess-2020-606
Preprint. Discussion started: 4 December 2020


Hydrology and Earth System Sciences
Discussions

(GLUE) technique is used to quantify GR4J parameter uncertainty. In assessing future flood hazard the sensitivity of results to different extreme value distributions is examined. In addition to evaluating each source of uncertainty independently, we use variance decomposition to quantify the contribution of each methodological choice and their interactions to the overall uncertainty in assessing flood risk. The climate change impact is evaluated based on relative future changes in the magnitude of floods for the 2020s (2010-2039), 2050s (2040-2069) and 2080s (2070-2099) with respect to the reference period (1976-2005). The following sections provide further details on the study catchments and each stage of the modelling chain employed.

### 2.1 Study catchments and hydro-climate datasets

Simulations are undertaken for four catchments (Boyne, Blackwater, Newport and Slaney), each representing different flood response types across the Ireland as evaluated by Broderick et al. (2019). Their location, together with a summary of hydro-climatic conditions for each catchment is summarized in Table 1 and Figure 2. Catchment area ranges from 146 $km^2$ (Newport) to 2447 $km^2$ (Boyne), while elevation ranges from 56 m (Newport) to 112 m (Blackwater). For each catchment we use gridded (1 × 1 km) daily precipitation and temperature data (Walsh, 2012) area averaged for the period 1976-2005 to provide a single representative baseline series for each catchment. Daily potential evapotranspiration is derived using air temperature and elevation following the method of Hamon (1964). This approach is favored over less parsimonious but more physically based methods (e.g. Penman-Monteith), which have greater data input requirements (e.g. wind speed, humidity) not available for all study catchments. Daily discharge data for each catchment was obtained from the Office of Public Works (OPW) (**http://www.epa.ie/hydronet/**).

### 2.2 Climate Projections and Bias Correction

Daily precipitation (pr) and air temperature (tas) time series for the period 1971-2100 were extracted for 12 members of the CMIP6 ensemble (https://esgf-node.llnl.gov/search/cmip6/) forced by each of three Shared Socioeconomic Pathway (SSP) (SSP1, SSP3 and SSP5) scenarios (see Table 2 for details). For each catchment daily precipitation and air temperature were extracted from the closest land-based GCM grid overlying the catchment centroid. It is widely acknowledged that climate models exhibit biases in their outputs (Krinner & Flanner, 2018; Giorgi & Gao, 2018), with numerous studies highlighting the need to post-process climate model output before use in simulating hydrological response (Ehret et al., 2012; Teng et al., 2012; Osuch et al., 2015; Meresa & Romanowicz, 2017). However, there is still no consensus on which bias correction techniques are most effective, nor in how bias correction techniques can modify future climate change signals. For instance, Teutschbein & Seibert (2013) and Yang et al. (2010) showed distribution mapping based on theoretical distributions outperforms other bias correction methods. Similarly, Chen et al. (2013) and Berg et al. (2012) show that theoretical distribution mapping performs similar to, or marginally better than, empirical quantile mapping. On the contrary, Gudmundsson et al. (2012), Gutjahr & Heinemann, (2013) and Lafon et al. (2013), show that empirical quantile mapping demonstrates higher skill than theoretical distribution mapping in systematically correcting precipitation. Given these varied results, we employ five commonly used

https://doi.org/10.5194/hess-2020-606
Preprint. Discussion started: 4 December 2020


Hydrology and Earth System Sciences
Discussions

techniques to bias correct raw climate model output and to examine the contribution of the selected bias correction methods to the total uncertainty in future flood hazard.

### *2.2.1 Change factor /delta change (CF)*

The change factor technique applies multiplicative (for precipitation) and/or additive (for temperature) procedures for correcting raw model output. This involves correcting simulated daily precipitation ($P_{fut,corr}$) by multiplying the ratio of observed precipitation ($P_{obs}$) and reference precipitation simulation ($P_{ref,raw}$) to future simulations of raw climate model precipitation ($P_{fur,raw}$). For correcting future air temperature ($T_{fut,corr}$), the difference in observed air temperature ($T_{obs}$) and simulated temperature in the reference period ($T_{ref,raw}$) is added to raw climate output ($T_{fur,raw}$).

$$P_{fut,corr} = P_{fur,raw} * \frac{P_{obs}}{P_{ref,raw}} \quad (1)$$

$$T_{fut,corr} = T_{fur,raw} + (T_{obs} - T_{ref,raw}) \quad (2)$$

### *2.2.2 Empirical quantile mapping*

Empirical quantile mapping is based on pair-wise comparison between the empirical cumulative density functions (ecdf) of observed and simulated daily precipitation time series during the reference period (1976-2005). This is a purely empirical and direct matching of the histogram of the observed precipitation to the future period. Future precipitation and temperature are corrected using the inverse of the ecdf ($ecdf^{-1}$) and fitted ecdf $ecdf_{hst,m}$.

$$P_{hst,m}^{cor} = (ecdf_{obs,m}^{-1}(ecdf_{hst,m}(P_{hst,m}))) \quad (3)$$

$$T_{hst,m}^{cor} = (ecdf_{obs,m}^{-1}(ecdf_{hst,m}(T_{hst,m}))) \quad (4)$$

The non-parametric quantile matching was performed first in the reference period (m, modeling period) using an exponential transfer function assumption. Then the calibrated coefficients were used to correct the future daily precipitation and air temperature.

### *2.2.3 Distribution Quantile Mapping (DQM)*

Distribution quantile mapping is a distribution parameter dependant bias correction technique. The parameters are extracted by fitting Gamma distribution to observed and simulated time series data, and matching its corresponding quantiles from the

https://doi.org/10.5194/hess-2020-606
Preprint. Discussion started: 4 December 2020


Hydrology and Earth System Sciences
Discussions

observed and raw climate model output in the reference period (1976-2005) (Piani et al., 2010). We applied two types of DQM to correct climate biases: Single Gamma Distribution Quantile Mapping (SGDQM) and Double Gamma Distribution Quantile Mapping (DGDQM), together with the Birnbaum-Sanders distribution method (BSM) (Marzena Osuch et al., 2016). These methods also allow for the excess number of dry, drizzle and wet days to be considered and corrected. In the case of SGQM, the first step is fitting a Gamma distribution to the upper 75 % of daily observed and raw climate output precipitation distribution. Whereas in the DGDQM, the Gamma distribution is fitted to both the upper ≥ 75 % and to the lower < 75 % of the daily observed and raw climate output precipitation in the reference period (1976-2005). In both cases, non-rain days were removed and only wet days were considered. Similarly, BSM used the Birnbaum-Sanders distribution to transfer the precipitation quantile from the observed time series to raw output of the GCMs in the reference period.

$$P_{corr} = F_{dg}^{-1}(F_{dg}(P_{raw}(t), \alpha_{raw}, \beta_{raw}), \alpha_{Obs}, \beta_{Obs}) \quad (5)$$

$$P_{corr} = F_{db}^{-1}(F_{db}(P_{raw}(t), \alpha_{raw}, \beta_{raw}), \alpha_{Obs}, \beta_{Obs}) \quad (6)$$

$$T_{corr} = F_{db}^{-1}(F_{db}(T_{raw}(t), \alpha_{raw}, \beta_{raw}), \alpha_{Obs}, \beta_{Obs}) \quad (7)$$

$$T_{corr} = F_{dn}^{-1}(F_{dn}(T_{raw}(t), \alpha_{raw}, \beta_{raw}), \alpha_{Obs}, \beta_{Obs}) \quad (8)$$

Where $P_{corr}$ and $T_{corr}$ are the bias corrected daily precipitation and temperature, respectively. Likewise, $P_{raw}(t)$ and $T_{raw}(t)$ represent for raw climate model output for precipitation and temperature. The raw climate output inverse cumulative density (CDF) is symbolized by $F_{dg}^{-1}$, $F_{db}^{-1}$, and $F_{dn}^{-1}$ for precipitation and temperature, respectively. The dn, db and dg subscripts represent the normal (for temperature), Birnbaum-Sanders (for both precipitation and temperature) and Gamma (for precipitation) distributions, respectively. The Gamma (for precipitation) and Birnbaum-Sanders distributions have two parameters – the shape and scale parameters which are symbolised by α and β, and the normal (for temperature) distribution, with mean and standard deviation represented by μ and σ, respectively.

### 2.3 Bias correction performance evaluation

The performance of the selected bias correction techniques was evaluated using four statistical measures: Pearson Correlation (RR), Mean Absolute Error (MAE), Root Mean Square Error (RMSE) and Percent Bias (PBIAS). Evaluation was performed by comparing the ability of each approach to capture observed precipitation and temperature.

$$RR = \frac{\sum(P_S - \overline{P_S}) * (P_C - \overline{P_C})}{\sqrt{\sum(P_S - \overline{P_S})^2 * \sum(P_C - \overline{P_C})^2}} \quad (9)$$

https://doi.org/10.5194/hess-2020-606
Preprint. Discussion started: 4 December 2020


Hydrology and Earth System Sciences
Discussions

$$MAE = \frac{\sum_{i=1}^{n}|P_S - P_C|\text{^}2}{N} \quad (10)$$

$$PBIAS = \frac{\sum_{i=1}^{n}|P_S - P_C|}{\sum_{i=1}^{n} P_S} \quad (11)$$

$$RMSE = \left[\frac{\sum_{i=1}^{n}|P_S - P_C|^2}{N}\right]^{0.5} \quad (12)$$

Where Ps and Pc are observed and corrected precipitation, respectively, $\overline{P_C}$ is the mean of corrected precipitation, $\overline{P_S}$ the mean of observed precipitation and *N* is the number of observations.

### 2.4 Hydrological modelling

The GR4J model (Perrin et al., 2003) is a four parameter, lumped conceptual rainfall-runoff model that has been widely applied in different hydro-climate conditions (Meresa & Gatachew, 2019; Meresa et al., 2017; He et al., 2018). GR4J simulates streamflow using precipitation, temperature and evapotranspiration (Perrin et al., 2003). The model has two consecutive stores: one related to runoff production and the other to runoff routing. Detailed information about the model structure is given in Perrin et al. (2003). The upper and lower limits of the four model parameters are listed in Supplementary Table S1. The model was calibrated and validated using observations over the period 1976-2005. The first four years were used as a model warmup to stabilise the initial states of the hydrological parameters. Calibration was undertaken from 1981-1999 and validation from 2000-2005. The Nash Sutcliffe Efficiency (NSE) objective function was used to evaluate the model performance and to identify behavioural parameter sets (Nash and Sutcliffe, 1970). NSE is defined as:

$$NSE = 1 - \frac{\sum_{t=1}^{j}(Q_{o,t} - Q_{m,t})^2}{\sum_{t=1}^{j}(Q_{O,t} - \bar{Q}_o)^2} \quad (13)$$

where $Q_{o,t}$ and $Q_{m,t}$ are observed and simulated flow at time *t*, $Q_o$ is the mean observed flow and *j* is the length of the $j^{th}$ time series. The ability of hydrological model simulations to replicate the observations was further evaluated by deriving the proportion of extreme high flows inside the 95% confidence intervals (PCI). This is helpful for identifying a fixed NSE threshold for differentiating between behavioural and non-behavioural simulations (Li et al., 2011; Xu, 2014).

The Generalized Likelihood Uncertainty Estimation (GLUE) approach is widely applied to quantify hydrological model parameter uncertainty (Beven & Binley, 1992). GLUE is an informal statistical approach that uses Monte Carlo (MC) simulation to generate many possible hydrological parameter sets from specific ranges. In applying GLUE, we randomly generated 30,000 parameter sets (using a uniform distribution) from the ranges of each GR4J parameter. Behavioural parameter

https://doi.org/10.5194/hess-2020-606
Preprint. Discussion started: 4 December 2020


Hydrology and Earth System Sciences
Discussions

sets were identified based on the NSE (Equation 13) weighting efficiency function and PCI (Equation (14), with a resultant fixed threshold of NSE ≥ 0.5 employed.

$$PCI = \left[1 - \left|\left(\frac{NQ_{i,p}}{T} - 0.95\right)\right|\right] * \frac{1}{T} * \left(\sum \frac{L_{u,t,p} - L_{l,t,p}}{Q_{o,t}}\right) \quad (14)$$

where $L_{L,t,p}$ and $L_{U,t,p}$ are the lower and upper boundary values of the extreme flow CI, T is the sum of time steps, $Q_{o,t}$ is the observed extreme flow at time step $t$, $NQ_{in,p}$ is the number of extreme peak flow observations which fall within the extreme flow CI. The shape of the 95% CI is governed by the value of PCI; if PCI is closer to 0.95 more of the observed time series extremes fall in the confidence interval band.

## 2.5 Flood frequency analysis

Numerous extreme value distributions can be deployed to estimate the frequencies of high flows. For example, the Log-Pearson III distribution is very popular in the USA and Australia for infrastructure design (Griffis & Stedinger, 2007), the General Extreme Value and Pearson Type III distributions are widely used in Europe (Madsen et al., 2013), while the Wakeby and Log-Normal distributions have been frequently used in Asia (Chen et al., 2012). However, a single distribution model may not be able to capture the entire temporal and spatial variability of hydrological extremes. Therefore, we employ three common distribution types (LogN, Loglogistic and GEV) with Maximum Likelihood parameter estimator (MLE) for flood frequency curve development. MLE estimates the distribution parameters by optimising the likelihood function of the cumulative probability distribution density, and its reliability is evaluated using the standard error of the estimated parameters. These distributions were fitted to the annual maximum daily peak flow in each study catchment. In Equations 15- 17, the respective probability density function (PDF) of each distribution is presented. The GEV and Log-logistic models have three parameters, while the Log-Normal distribution has two parameters;

Log-Normal $$f(x) = \frac{\exp\left(-\frac{1}{2}\left(\frac{lnx-\mu}{\sigma}\right)^2\right)}{x\sigma\sqrt{2\pi}} \quad \sigma, \mu\ (\sigma>0) \quad (15)$$

Log Logistic $$f(x) = \frac{\beta\left(\frac{x}{\alpha}\right)^{\beta-1}}{\alpha[1+\left(\frac{x}{\alpha}\right)^{\beta}]^2} \quad (16)$$

GEV $$f(x) = \begin{cases} \frac{1}{\sigma}\exp\left(-(1+kz)^{\wedge-\frac{1}{k}}\right)(1+kz)^{-1-\frac{1}{k}} & k \neq 0 \\ \frac{1}{\sigma}\exp(-z-exp(-z)) & k = o \end{cases} \quad K, \sigma, \mu\ (\sigma>0) \quad (17)$$

Where, $\alpha$ is the scale parameter, $\beta$ is the shape parameter and $k$ is the location parameter.

https://doi.org/10.5194/hess-2020-606
Preprint. Discussion started: 4 December 2020


Hydrology and Earth System Sciences
Discussions

### 2.6 Uncertainty decomposition and estimation

We examine the relative contribution of four key components of the modelling chain to the projected uncertainty in future flood risk. These are climate models (CM), bias correction techniques (BC), hydrological model parameters (HP) and flood frequency distribution models (FF). For uncertainty decomposition, we only use a single SSP scenario (here SSP3), with the assumption that different studies will be interested in quantifying flood risk for different emissions outcomes separately. Unlike additive or multiplicative approaches to uncertainty estimation, ANOVA can decompose the aggregated source of uncertainty into individual components and their interaction using specific extreme flow indices (Meresa & Romanowicz, 2017). We develop a hypothesis test using an ANOVA model that can identify the effect of each component (CM, BC, HP, FF) in the model chain to the total variance of the extreme index (Y). According to n-way ANOVA principles, the model splits the total sum of squares (SST) into the sum of squares (SS) of the main variables and their interactions as follows:

$$SST = \sum_{i=1}^{NCM=12} \sum_{j=1}^{NBC=5} \sum_{k=1}^{NHP=300} \sum_{l=1}^{NFF=3} \left(Y_{ijkl} - \bar{Y}\right)^2 \quad (18)$$

Where $Y_{ijkl}$ is estimated flood magnitude considering i=12 climate models, j=5 bias correction methods, k=300 hydrological parameter sets, l=3 extreme frequency distributions, and $\bar{Y}$ is the mean of all variables. SST is a grand square deviation of the main and interacting variables. Further, the deviation in SST is split into the individual and interacting components to explore their effect on the aggregated extreme flood frequency indices as follows:

$$SST = SS_{CM} + SS_{BC} + SS_{HP} + SS_{FF} + SS_{CMBC} + SS_{CMHP} + SS_{CMFF} + SS_{BCHP} + SS_{BCFF} + SS_{HPFF} \quad (19)$$

where $SS_{CM}$ is the sum of standard errors of climate models, $SS_{BC}$ is the sum of standard errors of bias correction methods, $SS_{HP}$ the sum of standard errors of hydrological parameters and $SS_{FF}$ is the sum of the standard errors of flood frequency. In examining combined effects, $SS_{CMBC}$ is the sum of standard errors of climate models and bias correction methods, $SS_{CMFF}$ the sum of standard errors of climate models and extreme frequency, and $SS_{BCHP}$ is the sum of standard errors of bias correction methods and hydrological parameters.

## 3. Results

### 3.1 Evaluation of bias correction techniques

The annual maximum daily precipitation series from 12 GCMs were evaluated against observations for each catchment during the period 1976-2005 (reference period). RR, MAE, PBIAS and RMSE results for each catchment are presented in Figure 3 and Figure S1. Following bias correction, results indicate an improvement of the GCMs in reproducing observed annual maximum precipitation. However, the performance of each bias correction method is not uniform for all catchments and GCMs. MAE values range from 0 to 195, RMSE 0 to 40, PBIAS -65 to 40, and R ranges from -0.40 to 0.50. Overall, the distribution based bias correction methods performed better in reproducing observed maximum precipitation in these

https://doi.org/10.5194/hess-2020-606
Preprint. Discussion started: 4 December 2020


catchments. The smallest PBIAS is observed in the Boyne catchment and largest in the Newport catchment. Figure 4 shows the raw GCM outputs together with the results of the five bias correction methods applied to the CMIP6 ensemble in simulating monthly maximum precipitation for each catchment. The corrected monthly precipitation gives a wider spread in winter months (except DGQM and EQM techniques), relative to summer months. However, the ensemble spread is dependent on the bias correction method. DGQM and EQM methods result in a relatively narrower spread in monthly simulations, whereas SGQM, BSM and CF return a wide range of simulations (Figure 4).

The influence of each bias correction method on the magnitude of simulated changes in annual maximum precipitation for the 2050s (2040-2069) and 2080s (2070-2099) (relative to reference period: 1976-2005) was evaluated for each GCM SSP combination (Figure 5). Simulated changes from the same 12 GCMs using different bias correction approaches show substantial differences in the magnitude of changes in annual maximum precipitation. Generally, projected changes are smaller in the Slaney and Boyne using DG methods, whereas the changes in the Blackwater and Newport are smaller using EQ and SG. There is also a linear relationship between the annual maximum precipitation changes suggested for the 2050s and 2080s, indicating a positive trend in the magnitude of changes with time (Figure 5). We also note that the magnitude of change in annual maximum precipitation tends to be higher for SSP5 than for SSP3 and SSP1 and slightly higher in the Slaney and Newport catchments, relative to the Boyne and Blackwater.

A similar evaluation was undertaken for mean annual air temperature for each catchment. Figure 6 shows the bias corrected projected mean annual temperature for each catchment under each GCM/SSP combination, together with the ensemble median for each SSP. The selected catchments show continuous warming during the 21$^{st}$ century. The ensemble mean changes for SSP1, SSP3, and SSP5 scenarios are projected to be 10-12$^{o}$C, 11-13.3$^{o}$C, and 12-15$^{o}$C, respectively by the end of the century. The spread at the end of 21$^{st}$ century is somewhat wider than the earlier periods. Bias correction results for precipitation are shown in Figure S2 and for temperature in Figure S3.

### 3.2 Hydrological modelling and parameter uncertainty evaluation

Using the GR4J hydrological model, 30,000 parameter sets were randomly generated from uniform distributions with the NSE objective function threshold set to > 0.5, used to identify behavioural parameter sets. Figure 7 shows the seasonal maximum flow simulations derived using behavioural sets relative to observations for the years 1976-2005, together with the 90 percent confidence intervals of the simulations. Monthly maximum simulations mostly fall within the 95% and 5% confidence interval except in the Boyne catchment, where a portion of the observed maximum flow time series fall outside of the simulated confidence interval.

https://doi.org/10.5194/hess-2020-606
Preprint. Discussion started: 4 December 2020


Hydrology and Earth System Sciences
Discussions

Ensemble median projections of monthly maximum flow derived from 12 GCMs under SSP3 and 5 bias correction techniques for each catchment for the period 1976 to 2100 are shown in Figure 8. Increases are largest during the winter and early spring months in the Blackwater and Newport catchments, with maximum flow increasing from 17 $m^3/s$ to 25 $m^3/s$ during winter in the Newport catchment, and from 120 $m^3/s$ to 160 $m^3/s$ in the Blackwater. Also, the projected flows during late autumn and early summer periods shows the same trend and uniform pattern, with a maximum flow rate of about 35 $m^3/s$ for the Blackwater, 5 $m^3/s$ for Newport, 40 $m^3/s$ for the Boyne and 15 $m^3/s$ for the Slaney.

Percent changes in maximum flow simulated using each of the 12 GCMs bias corrected by each of the five methods, together with the raw simulations are presented in Figure 9. A clear increase in flow is suggested using DGQM, SGQM, CF, EQM and BSM, however, the magnitude of simulated increases differs depending on bias correction approach and are not uniform across the selected catchments. Overall, distribution based bias correction models give smaller changes in annual maximum flow time series. This indicates that wet-day frequency correction is very important for understanding future annual maximum flow projections. Annual maximum flow changes using EQM gives a higher spread range and uncertainty. Changes in annual maximum flow are smallest in the Boyne catchment and largest in the Newport catchment. Changes in annual maximum flow are more constrained under SSP3 and SSP5, than SSP1 (Figure 9).

### 3.3 Flood hazard projections under varying climate conditions

To evaluate changes in flood frequency we use the Akaike Information Criteria (AIC) to identify the best fitting distribution type in the reference period and observed time series for each GCM projection and catchment. Figure 10 shows the estimated flood quantile values at different return periods (from 2 year to 100 year) using GEV, LogN and LogL distribution models, and associated 95% confidence intervals from 12 GCMs (under SSP3 scenario) bias corrected using the DGQM method over the full simulation period (1976-2100). Overall, the LogL distribution returned the smallest changes in flood quantiles and the narrowest uncertainty band, while the estimated quantile values using LogL tend to be the largest across each catchment. The GEV distribution gives the largest uncertainty ranges in flood quantiles in all catchments (Figure 10).

Flood quantile changes were also evaluated for each future period under SSP3 using the GEV distribution fitted to the median GR4J simulation combining all GCMs and bias correction methods (Figure 11 and Figure S4). Each catchment shows a significant increase in flood quantile magnitudes in the future. Overall, changes in flood quantiles are consistent with changes in annual maxima daily flow. However, future flood quantile changes are not the same across catchments and differences exist based on bias correction methods employed. The frequency of the larger return period flood (100-year flood) increases to higher than once in 20 years. The smallest changes (0-15%) in flood quantiles are observed in the Slaney using DGQM, the Boyne using SGQM and DGQM, Newport using CF and EQM, and in the Blackwater using CF. For the 100-year flood, the largest changes in magnitude (50-200%) are noted using EQM in the selected catchments. By comparison, the other bias correction methods are consistent and indicate changes of between 30-50% in the Slaney and Boyne, and 50-100% in

https://doi.org/10.5194/hess-2020-606
Preprint. Discussion started: 4 December 2020


Hydrology and Earth System Sciences
Discussions

330 Blackwater and Newport in the future. Overall, the Slaney catchment shows smaller relative change in flood quantiles (0-20%) at different return periods using BSM, SGQM and CF, similarly using the DGQM projected changes range from 0-15%. Moreover, changes in extreme flood quantiles do not increase linearly from the 2050s to 2080s. In almost all catchments and combinations of bias correction techniques changes are greater in the 2050s than the 2080s under SSP3.

### 3.4 Uncertainty estimation and decomposition for flood hazard estimation

335 The magnitude of each of the four sources of uncertainty on flood risk estimation was estimated first based on the additive chain principle to reveal their contribution to the overall uncertainty in projected changes. Projections from each of 12 climate models were iteratively passed through five bias correction techniques and used to force the GR4J model using behavioural parameters sets, before fitting each of the three frequency distributions to estimate future flood hazard. Figure 12 presents the integrative range of this cascade of uncertainty in estimating return period floods for each catchment using data spanning the 340 years 1976-2100. The dominant source of uncertainty differs from catchment to catchment. Climate models, flood frequency distribution and bias correction techniques tend to be the dominant contributing source of uncertainty in estimating flood quantiles. In the Newport and Blackwater catchments climate model projections present the dominant source of uncertainty, particularly for higher flood quantiles. Notably the relative magnitude of uncertainty in the smaller flood quantiles in the Blackwater catchment is different than for larger flood quantiles, with the extreme value distribution becoming dominant at 345 lower flood quantiles. The largest source of uncertainty in the Slaney is derived from the use of different frequency distribution models. For the Boyne catchment the bias correction methods contribute more to the total uncertainty. Therefore, the various steps in the modelling chain contribute differently in each catchment to total uncertainty in future flood risk estimation and in some catchments vary depending on the flood quantile of interest (Figure 12).

350 While additive chains may be useful for evaluating individual components of uncertainty, they do not allow identification of the interactive components of the uncertainty cascade. We use ANOVA to decompose the contribution of individual sources of uncertainty and their interaction in contributing to the total uncertainty in future flood hazard (Figure 13). We evaluate changes in 10-year, 50-year and 100-year return period flood for the 2080s (2070-2099) relative to the reference period (1976-2005). The decomposition of uncertainty is based on the variance in changes of flood quantile values and calculated out of 100 355 percent, i.e. the sum of all sources is equal to 100. The contribution of each source of uncertainty is not uniform across the selected catchments (Figure 13). Taking the example of the magnitude of the 100 year flood (Figure 13 outer band), future flood hazard in the Blackwater catchment for the 2080s is highly sensitive to the climate model used (36.5% of total uncertainty in 100-year flood) and respective bias correction methods (20% of total uncertainty). By contrast, future flood frequency in the Boyne is more sensitive to bias correction methods (30.0%) and extreme value distribution (25.5%) employed. In the 360 Boyne catchment, the climate model ensemble accounts for less than one quarter (22.5%) of the uncertainty in simulations of the 100-year flood by the 2080s and is comparable in magnitude to the interactive components of the cascade. In the Newport catchment the use of different extreme value distributions (36.3%) presents the largest component of uncertainty. The results

https://doi.org/10.5194/hess-2020-606
Preprint. Discussion started: 4 December 2020


Hydrology and Earth System Sciences
Discussions

of ANOVA analysis also confirm that the uncertainty resultant from the interaction of the key sources considered is not negligible and also varies on a catchment basis. In the Slaney and Blackwater catchments the interaction of various uncertainty components accounts for 16.8% and 16% of the total uncertainty in estimates of the 100-year flood by the 2080s. By contrast, interactive components in the Newport and Boyne catchments account for approximately one quarter of the uncertainty range (25.2% in the Newport and 22% in the Boyne). Overall, hydrological parameter uncertainty is the least dominant source of uncertainty in future flood frequency estimates across each catchment (Figure 12 and Figure 13). For estimates of the 100-year flood in the 2080s (Figure 13 outer band), hydrological model parameter uncertainty is typically 5% of the total uncertainty, reaching up to 9% in the Boyne. Furthermore, the contribution of each of the main components of uncertainty and their interactions to total uncertainty is broadly similar for the different return periods considered for our analysis of the 2080s (Figure 13).

## 4. Discussion

We examined future flood risk for four catchments in Ireland, including within our modelling chain the uncertainties derived from 12 CMIP6 GCMs, 5 commonly used bias correction techniques, hydrological model parameters and three flood frequency distributions. We found that maximum precipitation and mean air temperature in all catchments are projected to increase over the coming decades, however changes are not uniform across catchments. The largest change in annual maximum precipitation was found for the Newport catchment, with ensemble median increases becoming progressively larger for the 2020s, 2050s and 2080s (27%, 40%, 60%, respectively). In the Slaney catchment, increases in annual maximum precipitation between the 2050s and 2080s are not statistically significant. In the Blackwater catchment, most of the climate models indicate a positive change but these have a wide range of uncertainty relative to other catchments (from 0 to 55% in 2050s and 0 to 60% in 2080s). We find projected changes in flood magnitudes to be proportional to changes in maximum precipitation in all catchments. Projected changes in flood magnitude are higher using the SSP1 and SSP5 climate scenarios, whereas the SSP3 results in more modest flood increases. Overall changes in precipitation and air temperature are broadly consistent with previous findings using CMIP5 (Broderick et al., 2019) in Ireland.

Our findings demonstrate the large uncertainties associated with projected flood magnitudes. Over recent years much research has sought to explore the dominant sources of uncertainty in climate change impact assessments. For instance, Bastola et al. (2011b) identify hydrological model uncertainty as important in previous assessment of change in flood risk, others have identified climate models as being the dominant source (e.g. Sulis et al., 2012; Hattermann et al., 2018). Mizukami et al. (2016) rank hydrological model structure of greater importance than bias correction approaches in US catchments. However, our findings call into question the ability to generalise the most important components of the cascade of uncertainty in assessing future flood risk across catchments. Using variance decomposition to partition the components of the modelling chain employed, together with their interactions, we show that the dominant sources of uncertainty in assessing climate change

https://doi.org/10.5194/hess-2020-606
Preprint. Discussion started: 4 December 2020


Hydrology and Earth System Sciences
Discussions

impacts on future floods differ on a catchment by catchment basis. In two of our study catchments the extreme value distribution employed for flood frequency analysis and the bias correction method used to adjust raw GCM output contribute greater uncertainty to future flood risk than the ensemble of GCMs employed. Across all catchments the uncertainty in future hydrological model parameters is the smallest component of total uncertainty, while the contribution to total uncertainty from the interaction of components within the modelling chain is substantial – up to one quarter of the uncertainty range considered in two catchments.

While our sample is small, results suggest that rather than being the same across catchments, the dominant sources of uncertainty in future flood quantiles are catchment dependent. Vetter et al. (2017) used variance decomposition to examine the contribution of modelling chains (GCM, emissions scenario (in the form of Representative Concentration Pathways (RCPs)) and hydrological model) to total uncertainty in different parts of the flow regime. In their study they examine 12 large catchments globally. While Vetter et al. (2017) highlight the dominance of GCMs in total uncertainty across many catchments they highlight that the share of emissions scenario and hydrological model contributions to overall uncertainty can differ between catchments. Similar to our findings, Vetter et al. (2017) highlight the importance of interacting components of the modelling chain employed. The possibility that dominant sources of uncertainty differ on a catchment by catchment basis presents challenges for both top down and bottom up approaches to climate change adaptation. Top down approaches must a-priori decide on the components of the modelling chain to include. Including all relevant components is a very resource expensive task (Smith et al., 2018) and it may not be apparent at the outset which components of modelling chain to include for specific catchments. For bottom up approaches, such as the scenario neutral method (Broderick et al., 2019), the modeller is forced to choose which aspects of uncertainty to prioritise in assessing sensitivity to future changes. Again, this may not be apparent a priori. Moreover, the findings of Dobler et al. (2012) suggest that the dominant components of the modelling chain may further vary depending on which part of the flow regime (low, mean, high flows) is of interest. They highlight, for example, that the importance of bias correction approaches to the overall uncertainty in hydrological response increases for high flows. Our analysis of flood magnitudes for different return periods using all data from 1976-2100 suggests that the dominant source of uncertainty may also vary based on the return period of interest.

Our results show the value of ANOVA based methods for examining and visualising the relative contribution of uncertainties within the modelling chain considered. In our example we used the planning horizon of the 2080s to decompose uncertainties. In addition, the use of ANOVA techniques to quantify uncertainty may offer insight into where effort to reduce uncertainty may be most fruitful (Clark et al., 2016). In all catchments the magnitude of change in flood events is heavily dependent on the approach to bias correction. Across all catchments EQM performs the poorest at matching precipitation quantiles during the historical period. All other methods considered show consistent performance except in the Blackwater catchment. This is likely due to long positive tail of the precipitation distribution and intensity characteristics in the Blackwater. On the whole,

https://doi.org/10.5194/hess-2020-606
Preprint. Discussion started: 4 December 2020


Hydrology and Earth System Sciences
Discussions

430 distribution-based methods tend to be most consistent across the selected catchments and also have relatively smaller spread. Therefore, the DGQM or SGQM method (s) are promising for future risk evaluation and minimizing uncertainty.

Given the importance of uncertainty quantification in adapting to climate change it should be a priority for future work to examine how the dominant components of uncertainty in modelling chains relate to catchment characteristics. While our study
435 of four catchments is limited in this regard, there is evidence that catchment characteristics, which provide insight into the processes governing the rainfall runoff response, may also play a role in determining the components of the modelling chain that dominate uncertainties in future flood projections. The Newport catchment is the smallest of our sample (146 $Km^2$) and is an elevated catchment with a flashy response to rainfall. The shorter time of concentration and linear precipitation-runoff relationship mean that this catchment is highly sensitive to changes in extreme precipitation with uncertainty in flood frequency
440 distribution and bias correction accounting for over half of the total uncertainty in the projected 100 year flood in the 2080s. The Boyne catchment has been subject to significant arterial drainage works which have resulted in a faster rainfall runoff response and elevated high flows (Harrigan et al., 2020; Berghuijs et al., 2019). Our findings suggest that bias correction and flood frequency distribution are the dominant sources of uncertainty in the projected 100 year flood by the 2080s in this catchment. In the Blackwater and Slaney catchments groundwater contributes significantly to runoff and the catchments are
445 larger with typically well drained soils. In both catchments the climate model ensemble represents the dominant source of uncertainty.

As our study has shown, the evaluation of uncertainties and their interaction in future flood risk assessment with climate change is a critical step in understanding future impacts and informing adaptation decision making. However, results depend on the
450 modelling chain employed. The work presented here is illustrative rather than exhaustive. We do not, for example, include uncertainties in future flood estimates derived from different hydrological model structures, nor do we evaluate the transferability of parameter sets to represent future rainfall runoff response (e.g. Broderick et al. 2016). We also assume that flood processes remain stationary within the 30-year windows used to evaluate changes, while we also assume that other factors that can influence rainfall runoff response, such as land use change, remain unchanged from the calibration period used
455 to train our hydrological models.

## 5. Conclusions

This study evaluates changes in future flood magnitude with climate change for four Irish catchments using a modelling chain incorporating 12 GCMs comprising the CMIP6 ensemble, 5 bias correction techniques, hydrological model parameter
460 uncertainty and the use of extreme value distributions. Our findings suggest increasing flood risk over the coming decades in all catchments, with changes in flooding largely consistent with changes in maximum precipitation. However, uncertainties in future flood changes are large and increase with time and flood quantile. Using ANOVA, we decompose uncertainties in future

https://doi.org/10.5194/hess-2020-606
Preprint. Discussion started: 4 December 2020


Hydrology and Earth System Sciences
Discussions

flood quantiles to examine how individual components of the modelling chain and their interactions contribute to overall uncertainty. Our results show that the dominant sources of uncertainty vary on a catchment basis, calling into question the ability to generalise on the dominant components of uncertainty across catchments, even in a relatively small domain like Ireland. Across all four catchments the climate models, bias correlation methods and the extreme value distributions used to evaluate flood return periods were differentially dominant, while the uncertainty derived from the interaction of various components was substantial in all catchments. Hydrological model parameter uncertainty was the least important component. Our work shows the value of ANOVA methods in visualising and quantifying the uncertainty cascade at a catchment level which will be helpful in navigating the uncertainties associated with future flood risk for better adaptation decision making. While our sample is small, there is evidence that the dominant components of uncertainty in future flood risk may be related to catchment characteristics. Future work to better understand the link between the key components of the cascade of uncertainty and catchment characteristics is therefore recommended.

**Funding**

This work was made possible by the award of funding from the Office of Public Works and Kildare County Council to HM, CM and RF.

**Conflict of interest**

None

**References**

Bastola, S., Murphy, C., and Sweeney, J:.. The role of hydrological modelling uncertainties in climate change impact assessments of Irish river catchments. Advances in Water Resources, 34(5), 562–576. https://doi.org/10.1016/j.advwatres.2011.01.008, 2011a.

Bastola, S., Murphy, C., and Sweeney, J:. The sensitivity of fluvial flood risk in Irish catchments to the range of IPCC AR4 climate change scenarios. Science of the Total Environment, 409(24), 5403–5415. https://doi.org/10.1016/j.scitotenv.2011.08.042, 2011b.

Berg, P., Feldmann, H., and Panitz, H. J:. Bias correction of high resolution regional climate model data. Journal of Hydrology, 448–449, 80–92. https://doi.org/10.1016/j.jhydrol.2012.04.026, (2012).

Berghuijs, W. R., Harrigan, S., Molnar, P., Slater, L. J., and Kirchner, J. W:. The Relative Importance of Different Flood-

https://doi.org/10.5194/hess-2020-606
Preprint. Discussion started: 4 December 2020


Generating Mechanisms Across Europe. Water Resources Research, 55(6), 4582–4593. https://doi.org/10.1029/2019WR024841, (2019).

Beven, K., and Binley, A:. The future of distributed models: Model calibration and uncertainty prediction. Hydrological Processes, 6(3), 279–298. https://doi.org/10.1002/hyp.3360060305, (1992).

Blöschl, G., Hall, J., Parajka, J., Perdigão, R. A. P., Merz, B., Arheimer, B., Aronica, G. T., Bilibashi, A., Bonacci, O., Borga, M., Čanjevac, I., Castellarin, A., Chirico, G. B., Claps, P., Fiala, K., Frolova, N., Gorbachova, L., Gül, A., Hannaford, J., … Živković, N:. Changing climate shifts timing of European floods. Science, 357(6351), 588–590. https://doi.org/10.1126/science.aan2506, 2017.

Blöschl, G., Hall, J., Viglione, A., Perdigão, R. A. P., Parajka, J., Merz, B., Lun, D., Arheimer, B., Aronica, G. T., Bilibashi, A., Boháč, M., Bonacci, O., Borga, M., Čanjevac, I., Castellarin, A., Chirico, G. B., Claps, P., Frolova, N., Ganora, D., … Živković, N:. Changing climate both increases and decreases European river floods. Nature, 573(7772), 108–111. https://doi.org/10.1038/s41586-019-1495-6, (2019).

Broderick, C., Murphy, C., Wilby, R. L., Matthews, T., Prudhomme, C., and Adamson, M:. Using a Scenario-Neutral Framework to Avoid Potential Maladaptation to Future Flood Risk. Water Resources Research. https://doi.org/10.1029/2018WR023623, (2019).

Broderick, C., Murphy, C., Mooney, P., Matthews, T:. Changes in precipitation extremes for Ireland: Theoretical basis and future outlook. National Hydrology Conference, 2016.

Chen, J., Brissette, F. P., Chaumont, D., and Braun, M:. Finding appropriate bias correction methods in downscaling precipitation for hydrologic impact studies over North America. Water Resources Research, 49(7), 4187–4205. https://doi.org/10.1002/wrcr.20331, 2013.

Chen, L., Singh, V. P., Shenglian, G., Hao, Z., and Li, T:. Flood Coincidence Risk Analysis Using Multivariate Copula Functions. Journal of Hydrologic Engineering, 17(6), 742–755. https://doi.org/10.1061/(ASCE)HE.1943-5584.0000504, 2012.

Clark, M. P., Wilby, R. L., Gutmann, E. D., Vano, J. A., Gangopadhyay, S., Wood, A. W., Fowler, H. J., Prudhomme, C., Arnold, J. R., and Brekke, L. D:. Characterizing Uncertainty of the Hydrologic Impacts of Climate Change. Current Climate Change Reports, 2(2), 55–64. https://doi.org/10.1007/s40641-016-0034-x, 2016.

Dobler, C., Hagemann, S., Wilby, R. L., and StÃtter, J:. Quantifying different sources of uncertainty in hydrological projections in an Alpine watershed. Hydrology and Earth System Sciences, 16(11), 4343–4360. https://doi.org/10.5194/hess-16-4343-2012, 2012.

Ehret, U., Zehe, E., Wulfmeyer, V., Warrach-Sagi, K., and Liebert, J:. HESS Opinions "should we apply bias correction to global and regional climate model data?" Hydrology and Earth System Sciences, 16(9), 3391–3404. https://doi.org/10.5194/hess-16-3391-2012, 2012.

Fowler, H. J., Ekström, M., Blenkinsop, S., and Smith, A. P:. Estimating change in extreme European precipitation using a multimodel ensemble. Journal of Geophysical Research Atmospheres, 112(18). https://doi.org/10.1029/2007JD008619,


, 2007.

Giorgi, F., and Gao, X. J:. Regional earth system modeling: review and future directions. Atmospheric and Oceanic Science Letters, 11(2), 189–197. https://doi.org/10.1080/16742834.2018.1452520, (2018).

Griffis, V. W., and Stedinger, J. R:. Evolution of Flood Frequency Analysis with Bulletin 17. June, 283–297, 2007.

Gudmundsson, L., Wagener, T., Tallaksen, L. M., and Engeland, K:. Evaluation of nine large-scale hydrological models with respect to the seasonal runoff climatology in Europe. Water Resources Research, 48(11). https://doi.org/10.1029/2011WR010911, 2012.

Gutjahr, O., and Heinemann, G:. Comparing precipitation bias correction methods for high-resolution regional climate simulations using COSMO-CLM: Effects on extreme values and climate change signal. Theoretical and Applied Climatology, 114(3–4), 511–529. https://doi.org/10.1007/s00704-013-0834-z, 2013.

Gutmann, E. Pruitt, T. Clark, MP. Brekke, L. Arnold, JR. Raff, DA. and Rasmussen RM:. An intercomparison of statistical downscaling methods used for water resources assessments in the United States. Water Resour Res 50:7167–7186. doi:10.1002/ 2014WR015559, 2014.

Hamon, W. R:. Computation of direct runoff amounts from storm rainfall. In General Assembly of Berkeley, Symposium on Surface Waters: Vol. Extract of (pp. 52–62), 1964.

Harrigan, S., Zoster, E., Cloke, H., Salamon, P., and Prudhomme, C. Daily ensemble river discharge reforecasts and real-time forecasts from the operational Global Flood Awareness System. October, 1–22, 2020.

Hattermann, F. F., Vetter, T., Breuer, L., Su, B., Daggupati, P., Donnelly, C., Fekete, B., Florke, F., Gosling, S. N., Hoffmann, P., Liersch, S., Masaki, Y., Motovilov, Y., Muller, C., Samaniego, L., Stacke, T., Wada, Y., Yang, T., and Krysnaova, V:. Sources of uncertainty in hydrological climate impact assessment: A cross-scale study. Environmental Research Letters, 13(1). https://doi.org/10.1088/1748-9326/aa9938, 2018.

He, S., Guo, S., Liu, Z., Yin, J., Chen, K., and Wu, X:. Uncertainty analysis of hydrological multi-model ensembles based on CBP-BMA method. Hydrology Research, 49(5), 1636–1651. https://doi.org/10.2166/nh.2018.160, 2018.

Hughes, D. A., Kingston, D. G., & Todd, M. C:. Uncertainty in water resources availability in the Okavango River basin as a result of climate change. Hydrology and Earth System Sciences, 15(3), 931–941. https://doi.org/10.5194/hess-15-931-2011, 2011.

Iternational Panel on Climate Change (IPCC):. IPCC CLIMATE CHANGE 2013 Climate Change 2013. In Researchgate.Net. https://doi.org/10.1017/CBO9781107415324.Summary, 2013.

Kay, A. L., Davies, H. N., Bell, V. A., and Jones, R. G:. Comparison of uncertainty sources for climate change impacts: Flood frequency in England. Climatic Change, 92(1–2), 41–63. https://doi.org/10.1007/s10584-008-9471-4, 2009.

Knutti, R., and Sedláček, J:. Robustness and uncertainties in the new CMIP5 climate model projections. Nature Climate Change, 3(4), 369–373. https://doi.org/10.1038/nclimate1716, 2013.

Krinner, G., and Flanner, M. G:. Striking stationarity of large-scale climate model bias patterns under strong climate change. Proceedings of the National Academy of Sciences of the United States of America, 115(38), 9462–9466.


https://doi.org/10.1073/pnas.1807912115, 2018.

Lafon, T., Dadson, S., Buys, G., and Prudhomme, C:. Bias correction of daily precipitation simulated by a regional climate model: A comparison of methods. International Journal of Climatology, 33(6), 1367–1381. https://doi.org/10.1002/joc.3518, 2013.

Lawrence, D:. Uncertainty introduced by flood frequency analysis in projections for changes in flood magnitudes under a future climate in Norway. Journal of Hydrology: Regional Studies, 28(December 2019), 100675. https://doi.org/10.1016/j.ejrh.2020.100675, 2020.

Li, L., Xu, C. Y., Xia, J., Engeland, K., and Reggiani, P:. Uncertainty estimates by Bayesian method with likelihood of AR (1) plus Normal model and AR (1) plus Multi-Normal model in different time-scales hydrological models. Journal of Hydrology, 406(1–2), 54–65. https://doi.org/10.1016/j.jhydrol.2011.05.052, 2011.

Mazzorana, B., Levaggi, L., Keiler, M., and Fuchs, S:. Towards dynamics in flood risk assessment. Natural Hazards and Earth System Science, 12(11), 3571–3587. https://doi.org/10.5194/nhess-12-3571-2012, 2012.

Melsen, L. A., Teuling, A. J., Torfs, P. J. J. F., Zappa, M., Mizukami, N., Mendoza, P. A., Clark, M. P., and Uijlenhoet, R:. Subjective modeling decisions can significantly impact the simulation of flood and drought events. Journal of Hydrology, 568(November 2018), 1093–1104. https://doi.org/10.1016/j.jhydrol.2018.11.046, 2019.

Meresa, H.K., and Romanowicz, R. J:. The critical role of uncertainty in projections of hydrological extremes. Hydrology and Earth System Sciences, 21(8). https://doi.org/10.5194/hess-21-4245-2017, 2017.

Meresa, Hadush K., and Gatachew, M. T:. Climate change impact on river flow extremes in the upper blue nile river basin. Journal of Water and Climate Change, 10(4), 759–781. https://doi.org/10.2166/wcc.2018.154, 2019.

Meresa, H K., and Romanowicz, R. J:. The critical role of uncertainty in projections of hydrological extremes. Hydrology and Earth System Sciences. https://doi.org/10.5194/hess-21-4245-2017, 2017.

Meresa, H K, Romanowicz, R. J., and Napiorkowski, J. J:. Understanding changes and trends in projected hydroclimatic indices in selected Norwegian and Polish catchments. Acta Geophysica, 65(4), 829–848. https://doi.org/10.1007/s11600-017-0062-5, 2017.

Meresa, H K::. River flow characteristics and changes under the influence of varying climate conditions. Natural Resource Modeling, 33(1), 1–30. https://doi.org/10.1111/nrm.12242, 2020.

Mizukami, N., Clark, M. P., Gutmann, E. D., Mendoza, P. A., Newman, A. J., Nijssen, B., Livneh, B., Hay, L. E., Arnold, J. R., and Brekke, L. D:. Implications of the methodological choices for hydrologic portrayals of climate change over the contiguous united states: Statistically downscaled forcing data and hydrologic models. Journal of Hydrometeorology, 17(1), 73–98. https://doi.org/10.1175/JHM-D-14-0187.1, 2016.

Osuch, M., Romanowicz, R. J., Lawrence, D., and Wong, W. K:. Assessment of the influence of bias correction on meteorological drought projections for Poland. Hydrology and Earth System Sciences Discussions, 12(10), 10331–10377. https://doi.org/10.5194/hessd-12-10331-2015, 2015.

Osuch, Marzena, Romanowicz, R. J., Lawrence, D., and Wong, W. K:. Trends in projections of standardized precipitation


indices in a future climate in Poland. Hydrology and Earth System Sciences, 20(5), 1947–1969. https://doi.org/10.5194/hess-20-1947-2016, 2016.

Perrin, C., Michel, C., and Andréassian, V:. Improvement of a parsimonious model for streamflow simulation. Journal of Hydrology, 279(1–4), 275–289. https://doi.org/10.1016/S0022-1694(03)00225-7, 2003.

Piani, C., Haerter, J. O., and Coppola, E:. Statistical bias correction for daily precipitation in regional climate models over Europe. Theoretical and Applied Climatology, 99(1–2), 187–192. https://doi.org/10.1007/s00704-009-0134-9, 2010.

Prudhomme, C., Parry, S., Hannaford, J., Clark, D. B., Hagemann, S., and Voss, F:. How well do large-scale models reproduce regional hydrological extremes: In Europe? Journal of Hydrometeorology, 12(6), 1181–1204. https://doi.org/10.1175/2011JHM1387.1, 2011.

Rojas, R., Feyen, L., and Watkiss, P. Climate change and river floods in the European Union: Socio-economic consequences and the costs and benefits of adaptation. Global Environmental Change, 23(6), 1737–1751. https://doi.org/10.1016/j.gloenvcha.2013.08.006, 2013.

Saini, R., Wang, G., Yu, M., and Kim, J:. Phytoplankton light absorption and the package effect in relation to photosynthetic and photoprotective pigments in the northern tip of Antarctic Peninsula. Journal of Geophical Research, 3679–3699. https://doi.org/10.1002/2014JD022599, 2015.

Smith, K. A., Wilby, R. L., Broderick, C., Prudhomme, C., Matthews, T., Harrigan, S., and Murphy, C:. Navigating Cascades of Uncertainty — As Easy as ABC? Not Quite…. Journal of Extreme Events, 05(01), 1850007. https://doi.org/10.1142/s2345737618500070, 2018.

Soriano, E., Mediero, L., and Garijo, C:. Selection of bias correction methods to assess the impact of climate change on flood frequency curves. Water (Switzerland), 11(11). https://doi.org/10.3390/w11112266, 2019.

Steele-Dunne, S., Lynch, P., McGrath, R., Semmler, T., Wang, S., Hanafin, J., and Nolan, P:. The impacts of climate change on hydrology in Ireland. Journal of Hydrology, 356(1–2), 28–45. https://doi.org/10.1016/j.jhydrol.2008.03.025, 2008.

Sulis, M., Paniconi, C., Marrocu, M., Huard, D., and Chaumont, D:. Hydrologic response to multimodel climate output using a physically based model of groundwater/surface water interactions. Water Resources Research, 48(12), 1–18. https://doi.org/10.1029/2012WR012304, 2012.

Teng, J., Vaze, J., Chiew, F. H. S., Wang, B., and Perraud, J. M. Estimating the relative uncertainties sourced from GCMs and hydrological models in modeling climate change impact on runoff. Journal of Hydrometeorology, 13(1), 122–139. https://doi.org/10.1175/JHM-D-11-058.1, 2012.

Teutschbein, C., and Seibert, J:. Is bias correction of regional climate model (RCM) simulations possible for non-stationary conditions. Hydrology and Earth System Sciences, 17(12), 5061–5077. https://doi.org/10.5194/hess-17-5061-2013, 2013.

Vetter, T., Reinhardt, J., Flörke, M., Griensven, A. Van, Hattermann, F., Seidou, O., Su, B., and Vervoort, R. W:. Evaluation of sources of uncertainty in projected hydrological changes under climate change in 12 large-scale river basins. Climatic Change. https://doi.org/10.1007/s10584-016-1794-y, 2016.



Vetter, T., Reinhardt, J., Flörke, M., van Griensven, A., Hattermann, F., Huang, S., Koch, H., Pechlivanidis, I. G., Plötner, S., Seidou, O., Su, B., Vervoort, R. W., and Krysanova, V:. Evaluation of sources of uncertainty in projected hydrological changes under climate change in 12 large-scale river basins. Climatic Change, 141(3), 419–433. https://doi.org/10.1007/s10584-016-1794-y, 2017.

Walsh, S:. a Summary of Climate Averages. The Irish Meteorological Service, 582(417). www.met.ie, 2012.

Wilby, R. L., and Harris, I:. A framework for assessing uncertainties in climate change impacts: Low-flow scenarios for the River Thames, UK. Water Resources Research, 42(2), 1–10. https://doi.org/10.1029/2005WR004065, 2006.

Wilby, R., Murphy, C., Wilby, R., and Murphy, C:. Decision-Making by Water Managers Despite Climate Uncertainty. In The Oxford Handbook of Planning for Climate Change Hazards (Issue February). https://doi.org/10.1093/oxfordhb/9780190455811.013.52, 2019.

Wilby, R.L. and Dessai, S:. Robust adaptation to climate change. Weather, 65(7), pp.180-185, 2010.

Wyser, K., van Noije, T., Yang, S., von Hardenberg, J., O'Donnell, D., and Döscher, R. On the increased climate sensitivity in the EC-Earth model from CMIP5 to CMIP6. Geoscientific Model Development Discussions, November, 1–13. https://doi.org/10.5194/gmd-2019-282, 2019.

Xu, L. L. C:. The comparison of sensitivity analysis of hydrological uncertainty estimates by GLUE and Bayesian method under the impact of precipitation errors. 491–504. https://doi.org/10.1007/s00477-013-0767-1, 2014.

Yang, W., Andréasson, J., Graham, L. P., Olsson, J., Rosberg, J., and Wetterhall, F. Distribution-based scaling to improve usability of regional climate model projections for hydrological climate change impacts studies. Hydrology Research, 41(3–4), 211–229. https://doi.org/10.2166/nh.2010.004, 2010.

https://doi.org/10.5194/hess-2020-606
Preprint. Discussion started: 4 December 2020


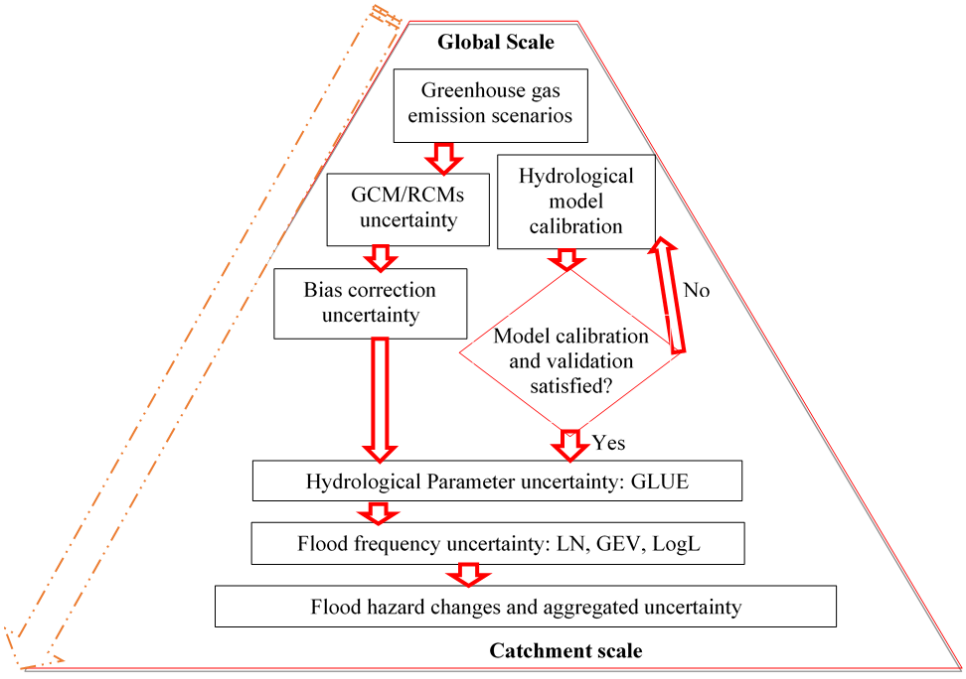


**Figure 1.** Research flow chart to estimate projections of flood hazard and identify associated uncertainty

https://doi.org/10.5194/hess-2020-606
Preprint. Discussion started: 4 December 2020


Hydrology and Earth System Sciences
Discussions

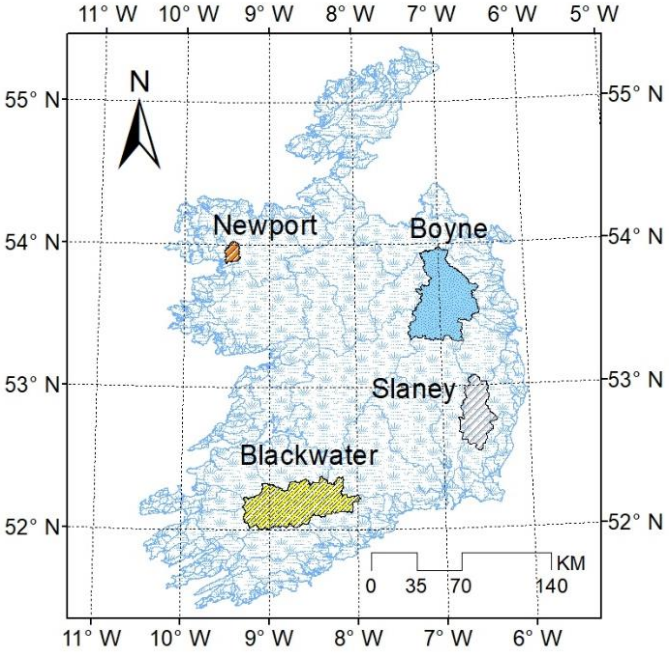


670 **Figure 2.** Location of the selected study catchments.

https://doi.org/10.5194/hess-2020-606
Preprint. Discussion started: 4 December 2020


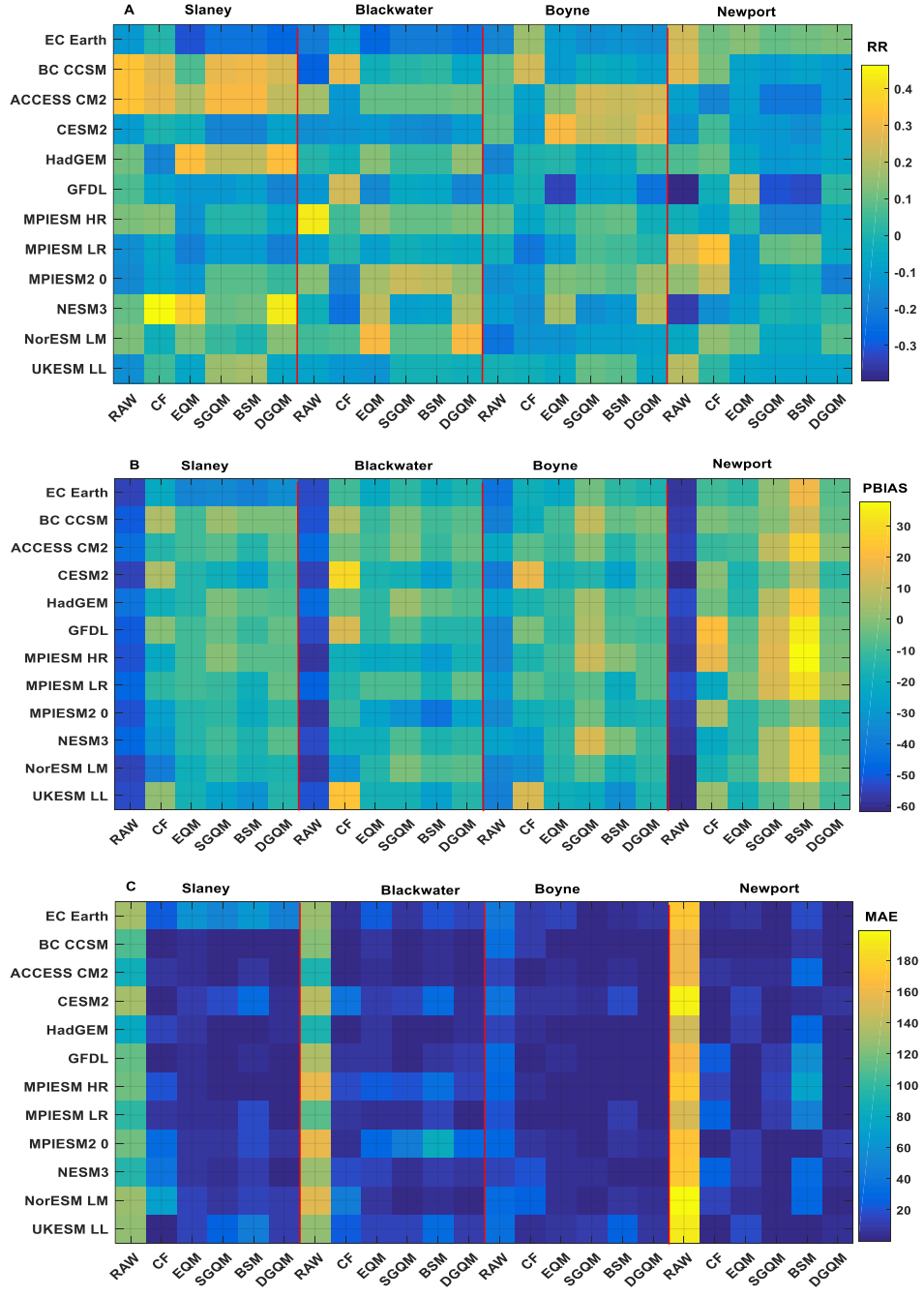


**Figure 3** Comparison of corrected annual maximum precipitation using five bias correction methods and observed annual maximum precipitation using a) Pearson correlation coefficient (RR), b) Percent Bias (PBIAS) and c) Mean Absolute Error (MAE). The y-axis indicates each of 12 CMIP6 climate models and the x-axis represents each of 5 climate bias correction method.

https://doi.org/10.5194/hess-2020-606
Preprint. Discussion started: 4 December 2020


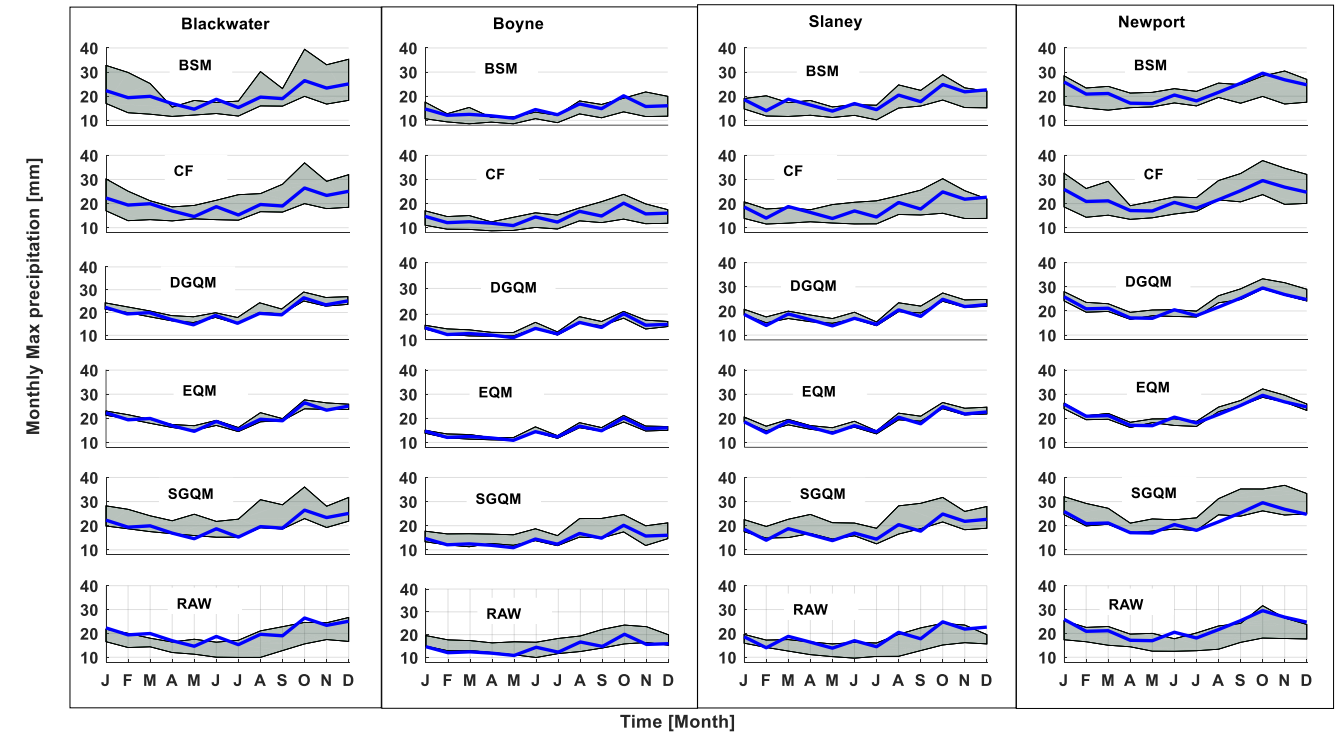


**Figure 4** Comparison of raw and bias corrected simulations from 12 CMIP6 GCMs with observed monthly maximum precipitation for each of our four study catchments. Each row presents results of one of five bias correction techniques (top row - Birnbaum Distribution (BSM), second row-Change Factors (CF), third row- Double Quantile Mapping using Gamma Distribution (DGQM), fourth row-Empirical Quantile Mapping using Simple Interpolation (EQM), fifth row- Single Quantile Mapping using Gamma Distribution (SGQM), and the last row is the raw GCMs output). In each panel the grey shaded region represents the spread of 12 GCM simulations, with blue line being the observed monthly maximum precipitation.

https://doi.org/10.5194/hess-2020-606
Preprint. Discussion started: 4 December 2020


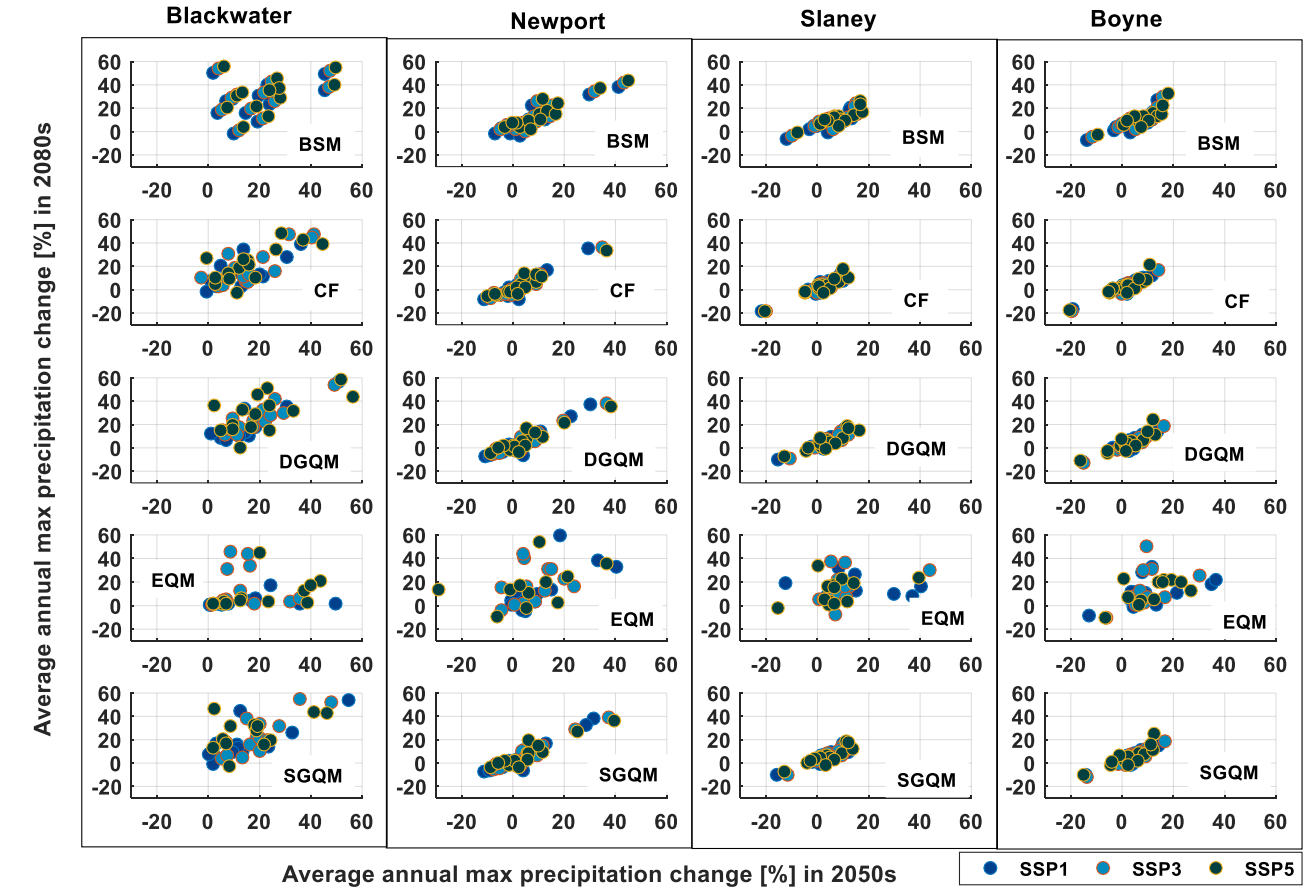


695 **Figure 5.** Scatter plots of change in maximum annual precipitation as simulated by 12 CMIP6 GCMs (each circle dot) corrected using each of the five bias correction techniques for three SSP scenarios for the 2050s (2040-2069) and 2080s (2070-2099). The dark blue circle represents SSP1, light blue represents SSP3 and dark green represents SSP5.

https://doi.org/10.5194/hess-2020-606
Preprint. Discussion started: 4 December 2020


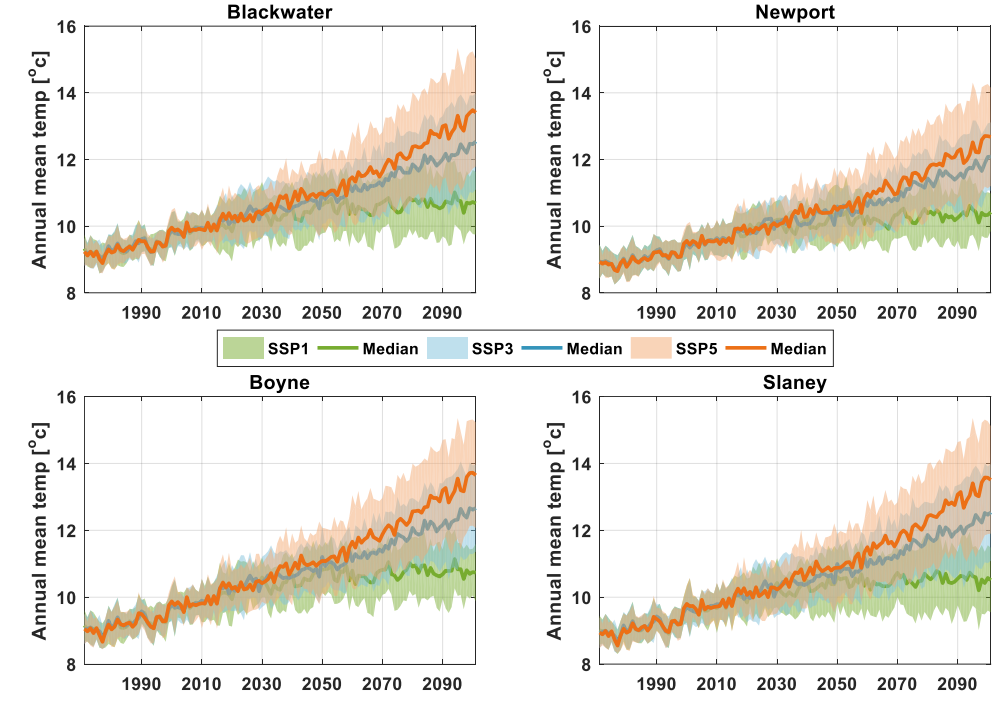


**Figure 6.** Ensemble of bias corrected simulations of annual mean air temperature (temp) from 12 CMIP6 GCMs for each catchment for the period 1976-2100. Orange, blue and green shaded areas represent the spread of GCM simulations forced using SSP1, SSP3 and SSP5, respectively. The solid lines represent the median of the 12 GCMs for each SSP scenario.

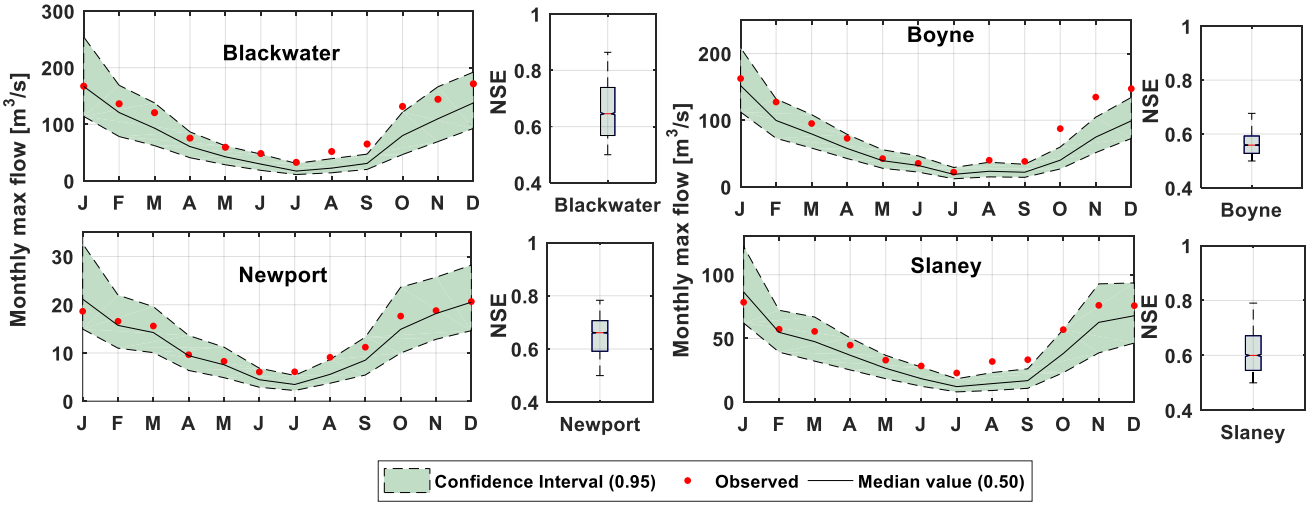


**Figure 7.** Observed and simulated monthly maximum flows ($m^3/s$) using GR4J behavioural parameter sets for the reference period (1976-2005). The black line and shaded area represent the median and 95 percent confidence interval of simulated flows, respectively, the red dot represents observed monthly maxima. Boxplots show the spread in NSE scores for behavioural parameters sets in each catchment.

https://doi.org/10.5194/hess-2020-606
Preprint. Discussion started: 4 December 2020




Hydrology and Earth System Sciences
Discussions

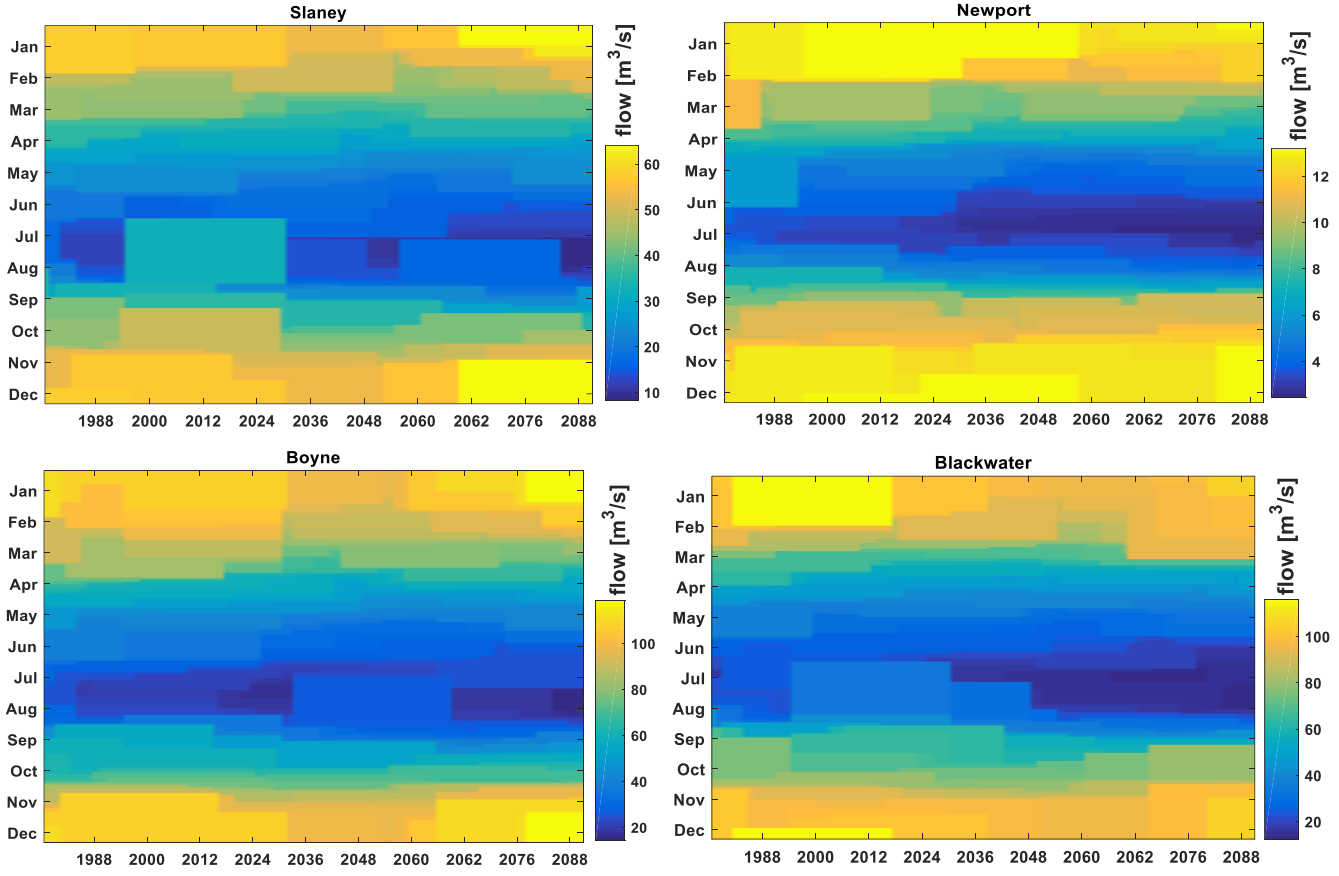


**Figure 8.** Ensemble median monthly maximum flow ($m^3/s$) projections for 1976-2100 in each catchment as simulated using 12 CMIP6 GCMs, the five bias correction techniques and the best parameter sets of the hydrological model.

https://doi.org/10.5194/hess-2020-606
Preprint. Discussion started: 4 December 2020


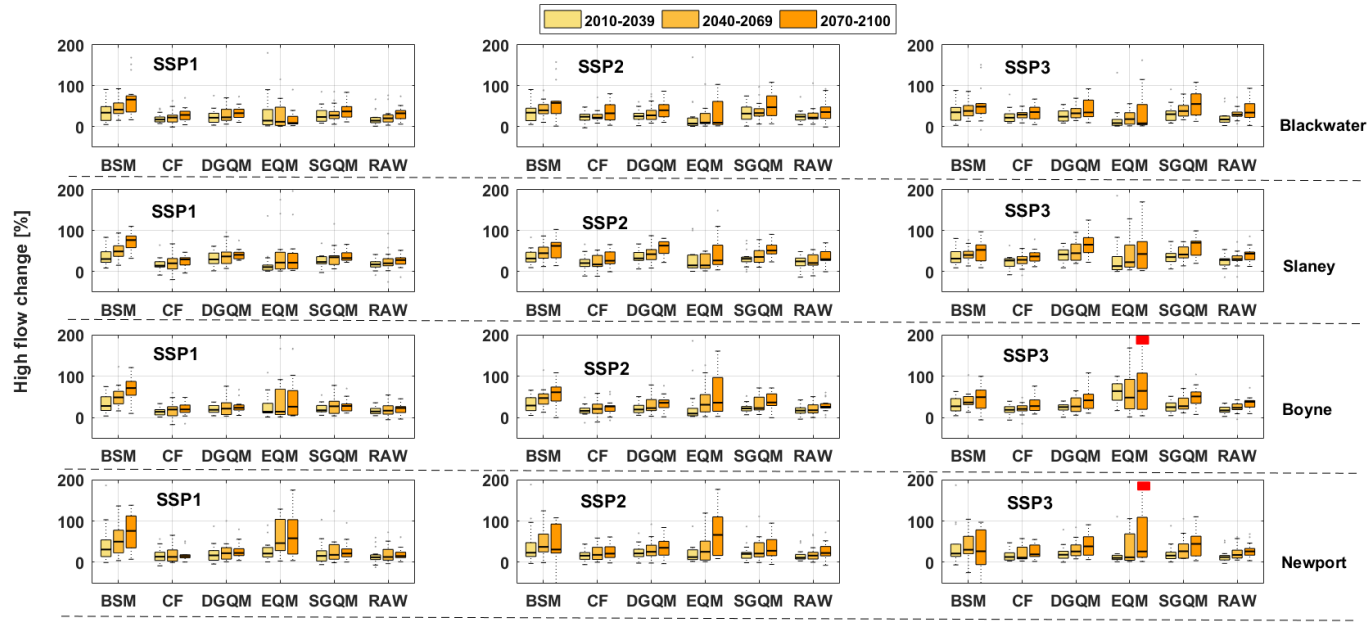


**Figure 9.** Matrix of projected percent changes in annual maximum river flow for the 2020s (2010-2039), 2050s (2040-2069), and 2080s (2070-2099) for SSP1, SSP3 and SSP5 in each catchment with respect to the reference period (1976-2005). Each box plot represents the spread of 12 GCMs for each of the five bias correction techniques as simulated using behavioural model parameter sets. Marked for each boxplot are the median and 0.25 and 0.75 quantiles. The red dots are outliers (changes above 200%).

https://doi.org/10.5194/hess-2020-606
Preprint. Discussion started: 4 December 2020


Hydrology and Earth System Sciences
Discussions

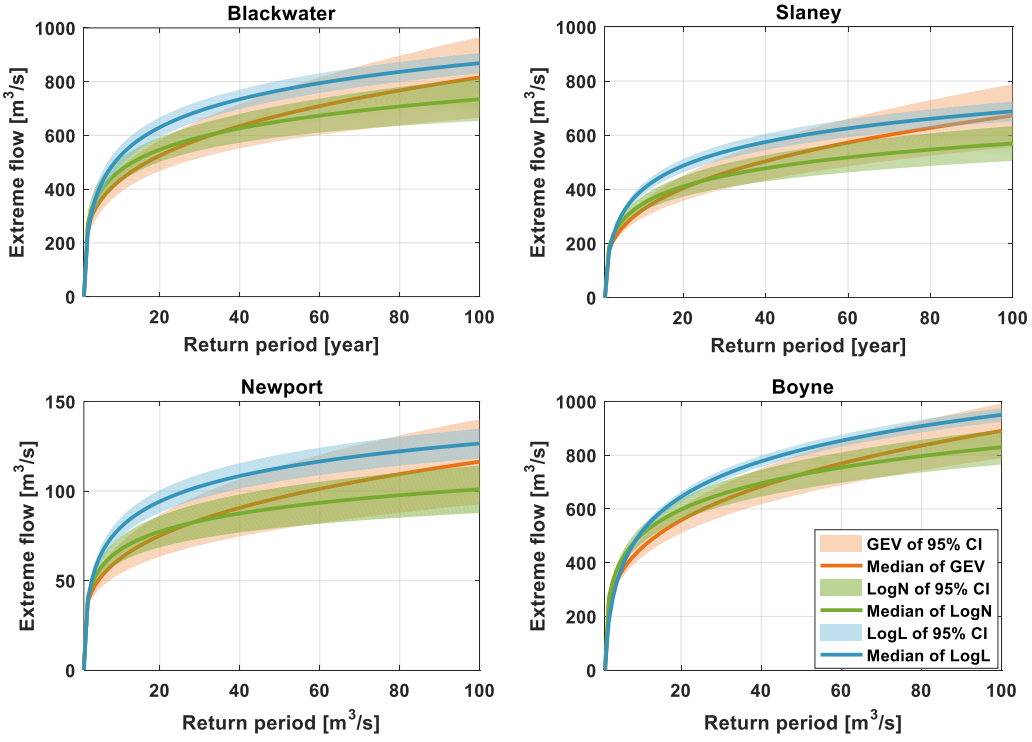


725 **Figure 10.** Comparison of flood quantiles estimated using three flood distribution models (LogL, GEV and LogN) fitted to projected annual maxima series using derived from 12 GCMs bias corrected using the DGQM method. The shaded region indicates the 95% confidence interval of annual maximum projections from 12 GCMs under SSP3 scenario during full projection period (1970-2100 period) in each catchment.

730

https://doi.org/10.5194/hess-2020-606
Preprint. Discussion started: 4 December 2020


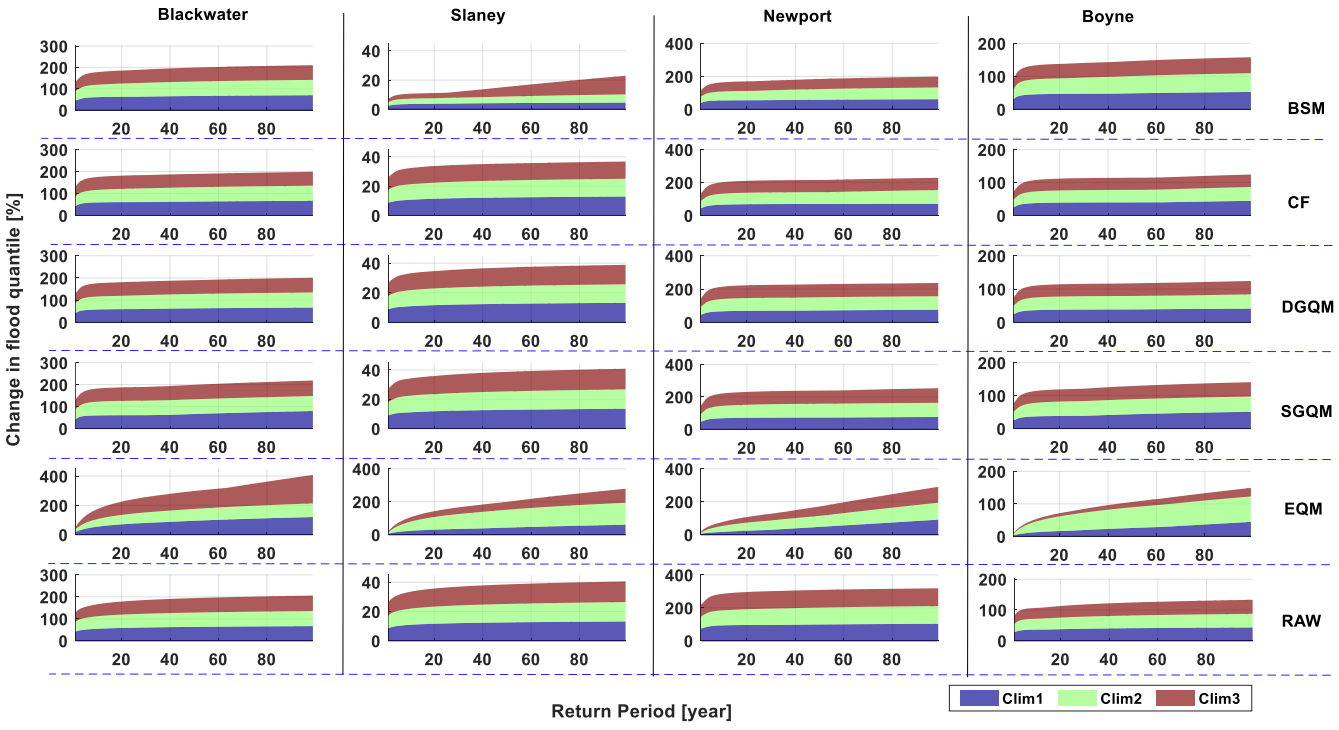


**Figure 11.** Percent changes in extreme flow quantiles using ensemble of three distribution types in each catchment for the 2020s (clim1), 2050s (clim2) and 2080s (clim3). Simulated changes are derived using raw (bottom row) and bias corrected (the first four rows) simulations. The shaded region is the spread of 12 climate model and three flood frequency models in the 2020s (blue), 2050s (green) and 2080s (brown) period.

https://doi.org/10.5194/hess-2020-606
Preprint. Discussion started: 4 December 2020


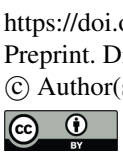

Hydrology and Earth System Sciences
Discussions
Open Access
EGU

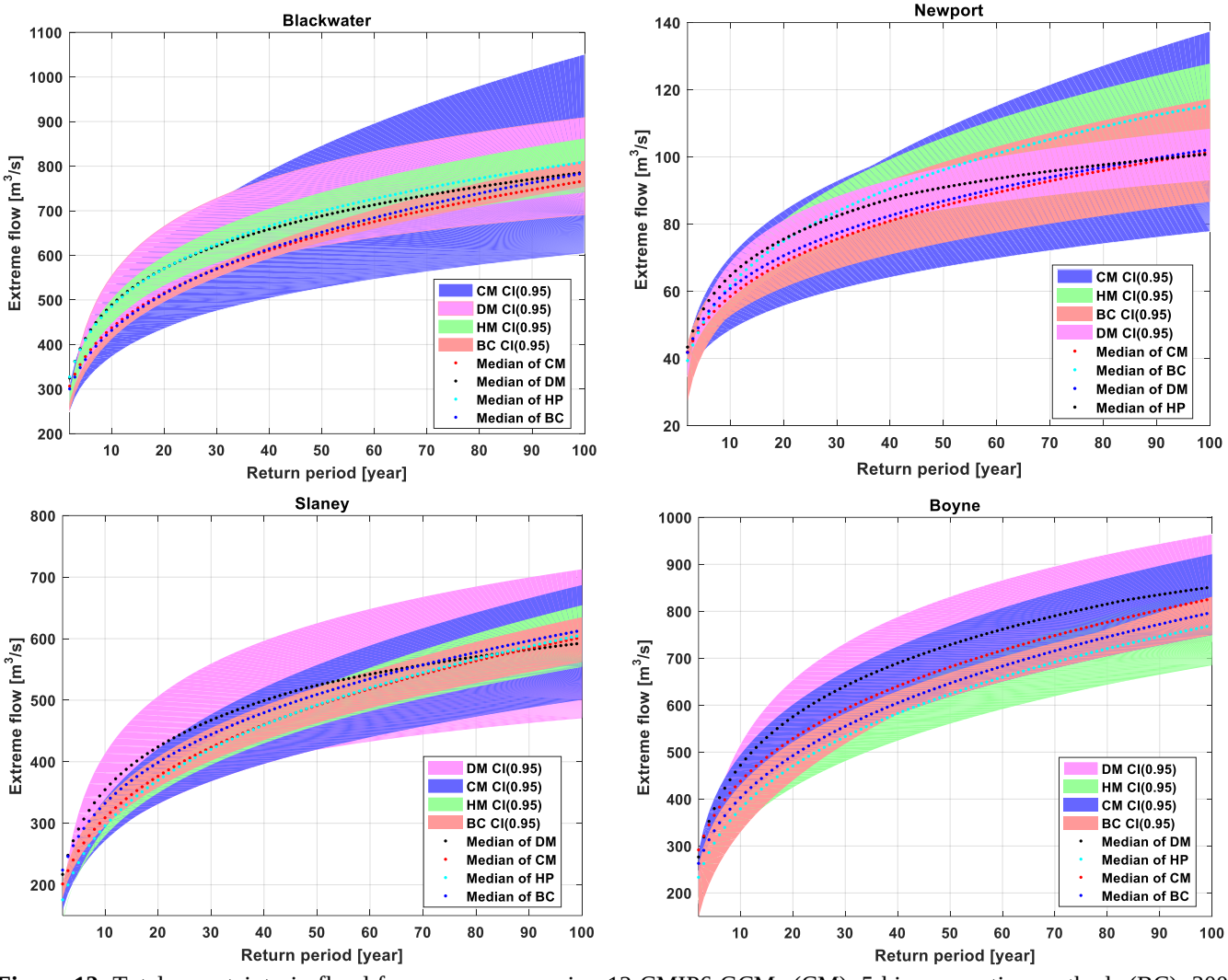


**Figure 12.** Total uncertainty in flood frequency curve using 12 CMIP6 GCMs (CM), 5 bias correction methods (BC), 300 behavioural parameter sets (HM) and 3 extreme value distributions (DM). Shaded areas represent the 95 percent confidence interval for each component in the modelling chain while the dotted line stands for their respective median values. The curves are fitted to annual maximum time series derived for 1976-2100.

https://doi.org/10.5194/hess-2020-606
Preprint. Discussion started: 4 December 2020


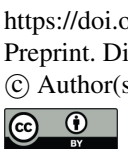

Hydrology and Earth System Sciences
Discussions

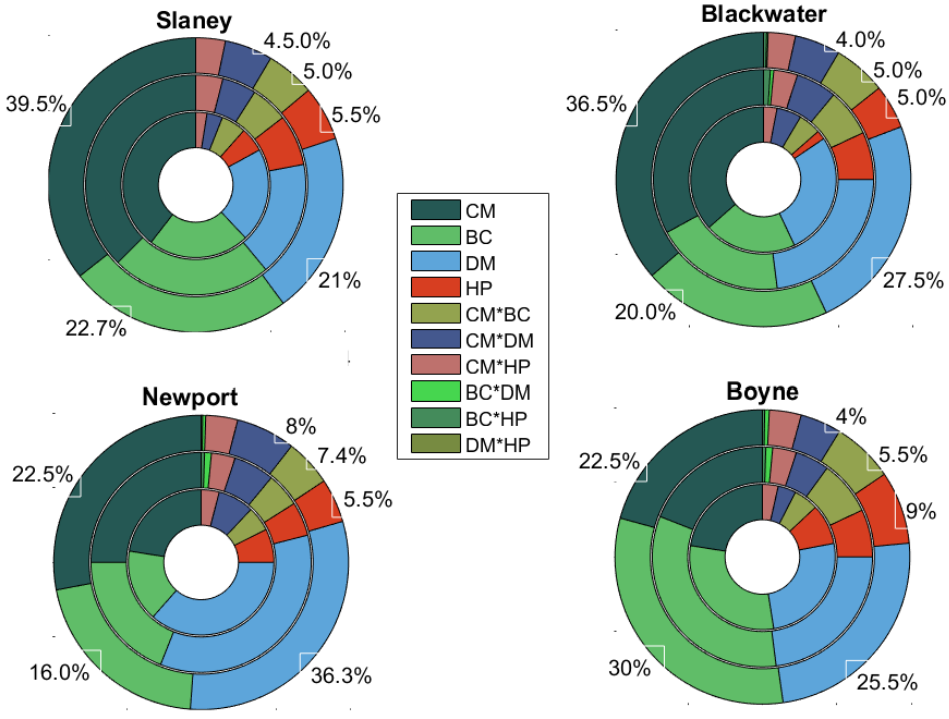


**Figure 13.** Contribution of each component of the modelling chain, together with their interaction, to the range of simulated changes in flood risk for the 2080s (2070-2099) relative to the reference period (1976-2005). Sources considered include 12 CMIP6 climate models (CM), 5 bias correction techniques (BC), hydrological model parameter uncertainty (HP) and 3 extreme value distribution models (DM). The outermost circle/donut represents the flood quantile change at return period (RP) of 100 years, the middle circle RP of 50 years and innermost circle RP of 10 years for the 2080s. Percent changes are annotated for the outermost circle (100-year flood).

https://doi.org/10.5194/hess-2020-606
Preprint. Discussion started: 4 December 2020


Hydrology and Earth System Sciences
Discussions

**Table 1.** Statistical and hydro-climatic characteristics of each study catchment.

| | Boyne | Blackwater | Slaney | Newport |
|---|---|---|---|---|
| Latitude [degree] | 53.60 | 52.14 | 52.8 | 53.95 |
| Longitude [degree] | -6.96 | -8.94 | -6.61 | -9.44 |
| Catchment Area [$km^2$] | 2447.36 | 1257.20 | 1032.68 | 146.02 |
| Elevation [m] | 70.00 | 116.00 | 107.00 | 56.00 |
| 95% of river flow value [$m^3/s$] | 95.42 | 144.64 | 68.76 | 14.20 |
| Annual max flow [$m^3/s$] | 379.09 | 351.06 | 247.30 | 33.40 |
| 95% of precipitation value [mm] | 17.38 | 24.46 | 24.09 | 25.45 |
| Mean Annual max precipitation [mm] | 45.28 | 61.76 | 71.69 | 93.48 |
| Coefficient of Variance of river flow [monthly] | 0.94 | 0.75 | 0.82 | 0.56 |
| Median of annual maximum flow[$m^3/s$] | 214.83 | 220.65 | 135.51 | 24.60 |
| Coefficient of Variance of precipitation [monthly] | 0.49 | 0.47 | 0.53 | 0.45 |
| Base flow index [-] | 0.724 | 0.624 | 0.73 | 0.69 |
| Mean of surface runoff [$m^3/s$] | 10.21 | 13.14 | 5.77 | 1.86 |
| Mean of base flow [$m^3/s$] | 26.85 | 21.781 | 15.584 | 4.19 |

https://doi.org/10.5194/hess-2020-606
Preprint. Discussion started: 4 December 2020


Hydrology and Earth System Sciences
Discussions

**Table 2** List of CMIP6 climate models employed in this study

| Code | Institute | Parent source Id | Institution Id |
|---|---|---|---|
| CM1 | Commonwealth Scientific and Industrial Research Organisation, Australia | ACCESS-CM2 | CSIRO |
| CM2 | Beijing Climate Center, China | BCC-CSM2-MR | BCC |
| CM3 | National Center for Atmospheric Research, USA | CESM2 | NCAR |
| CM4 | European: EC-EARTH consortium | EC-Earth | EC-EARTH consortium |
| CM5 | Global Fluid Dynamics Laboratory, USA | GFDL | NOAA-GFDL |
| CM6 | Met Office Hadley Centre, UK | HadGEM3-GC31-LL | MOHC |
| CM7 | JAMSTEC, AORI, NIES, and R-CCS, Japan | MIROC6 | MIROC |
| CM8 | Max Planck Institute for Meteorology, Germany | MPI-ESM1-2-HR | MPI-M |
| CM9 | Meteorological Research Institute, Japan | MRI-ESM2-0 | MRI |
| CM10 | Nanjing University of Information Science and Technology, China | NESM3 | NUIST |
| CM11 | NorESM Climate modeling Consortium, Norway | NorESM2-LM | NCC |
| CM12 | Met Office Hadley Centre, UK | UKESM1-0-LL | MOHC |